NRC Research Press

ARTICLE

Combining satellite lidar, airborne lidar, and ground plots to estimate the amount and distribution of aboveground biomass in the boreal forest of North America[1]

Hank A. Margolis, Ross F. Nelson, Paul M. Montesano, André Beaudoin, Guoqing Sun, Hans-Erik Andersen, and Michael A. Wulder

Abstract: We report estimates of the amount, distribution, and uncertainty of aboveground biomass (AGB) of the different ecoregions and forest land cover classes within the North American boreal forest, analyze the factors driving the error estimates, and compare our estimates with other reported values. A three-phase sampling strategy was used (*i*) to tie ground plot AGB to airborne profiling lidar metrics and (*ii*) to link the airborne estimates of AGB to ICESat-GLAS lidar measurements such that (*iii*) GLAS could be used as a regional sampling tool. We estimated the AGB of the North American boreal forest at 21.8 Pg, with relative error of 1.9% based on 256 GLAS orbits (229 086 pulses). The distribution of AGB was 46.6% for western Canada, 43.7% for eastern Canada, and 9.7% for Alaska. With a single exception, relative errors were under 4% for the three regions and for the major cover types and under 10% at the ecoregion level. The uncertainties of the estimates were calculated using a variance estimator that accounted for only sampling error, i.e., the variability among GLAS orbital estimates, and airborne to spaceborne regression error, i.e., the uncertainty of the model coefficients. Work is ongoing to develop robust statistical techniques for integrating other sources of error such as ground to air regression error and allometric error. Small ecoregions with limited east–west extents tended to have fewer GLAS orbits and a greater percent sampling error. AGB densities derived from GLAS agreed closely with the estimates derived from both forest inventories (<17%) and a MODIS-based interpolation technique (<26%) for more southern, well-inventoried ecoregions, whereas differences were much greater for unmanaged northern and (or) mountainous ecoregions.

Key words: aboveground biomass, lidar, North American boreal forest, ICESat-GLAS, Landsat, MODIS, forest inventory, *k*NN.

Résumé : Nous présentons les estimations de quantité, distribution et incertitude de la biomasse aérienne de différentes régions écologiques et de différentes classes de couverts forestiers en Amérique du Nord, analysons les facteurs contrôlant les erreurs d'estimation, et comparons nos résultats avec ceux de la littérature. Un dispositif d'échantillonnage en trois étapes a été utilisé (*i*) pour associer la biomasse mesurée dans des placettes d'inventaire aux profils de lidar aéroporté et (*ii*) pour relier les estimations lidar aéroporté de biomasse aux mesures d'ICESat-GLAS, de sorte que (*iii*) GLAS puisse être utilisé comme outil d'échantillonnage régional. À partir de 156 orbites GLAS (229 086 impulsions), nous avons estimé la biomasse aérienne de la forêt boréale d'Amérique du Nord à 21.8 Pg avec une erreur relative de 1.9 %. La distribution de la biomasse aérienne était de 46.6 % pour l'ouest du Canada, 43.7 % pour l'est du Canada, et 9.7 % pour l'Alaska. Avec une seule exception, les erreurs relatives étaient inférieures à 4 % pour les trois régions et pour les principaux types de couvert, et inférieures à 10 % à l'échelle des régions écologiques. L'incertitude des estimations a été calculée via un estimateur de variance qui a seulement pris en compte l'erreur d'échantillonnage, c'est-à-dire la variabilité entre les estimations orbitales de GLAS, et l'erreur de la régression de l'estimation aéroportée sur les mesures satellitaires, c'est-à-dire l'incertitude des coefficients du modèle. Les travaux se poursuivent pour développer des techniques statistiques robustes pour intégrer d'autres sources d'erreur telles que l'erreur de régression de l'estimation au sol sur l'estimation aéroportée et des erreurs allométriques. De petites régions écologiques ayant une étendue est–ouest limitée ont généralement observé moins d'orbites GLAS et donc un pourcentage d'erreur d'échantillonnage plus élevé. Les densités de biomasse aérienne obtenues par GLAS correspondaient étroitement aux estimations dérivées des inventaires forestiers (<17 %) et d'une technique d'interpolation basée sur MODIS (<26 %) pour des régions écologiques méridionales bien inventoriées, tandis que les différences étaient bien plus importantes pour les régions montagneuses et (ou) septentrionales non aménagées.

Mots-clés : biomasse aérienne, lidar, forêt boréale nord-américaine, ICESat-GLAS, Landsat, MODIS, inventaire forestier, *k*NN.

Received 6 January 2015. Accepted 14 April 2015.

H.A. Margolis. Centre d'étude de la forêt, Faculté de foresterie, de géographie et de géomatique, Université Laval, Québec, QC G1V 0A6, Canada; Biospheric Sciences Laboratory, NASA Goddard Space Flight Center, Greenbelt, MD 20771, USA.
R.F. Nelson. Biospheric Sciences Laboratory, NASA Goddard Space Flight Center, Greenbelt, MD 20771, USA.
P.M. Montesano. Biospheric Sciences Laboratory, NASA Goddard Space Flight Center, Greenbelt, MD 20771, USA; Science Systems and Applications Inc., NASA Goddard Space Flight Center, Greenbelt, MD 20771 USA.
A. Beaudoin. Laurentian Forestry Centre, Canadian Forest Service, Natural Resources Canada, 1055 rue du PEPS, Québec, QC G1V 4C7, Canada.
G. Sun. Biospheric Sciences Laboratory, NASA Goddard Space Flight Center, Greenbelt, MD 20771, USA; University of Maryland, Department of Geographical Sciences, College Park, MD 20742, USA.
H.-E. Andersen. USDA Forest Service, Pacific Northwest Research Station, P.O. Box 352100, Seattle, WA 98195-2100, USA.
M.A. Wulder. Pacific Forestry Centre, Canadian Forest Service, Natural Resources Canada, 506 West Burnside Road, Victoria, BC V8Z 1M5, Canada.
Corresponding author: Hank A. Margolis (e-mail: Hank.Margolis@sbf.ulaval.ca).

Introduction

Extending east to west across the entire continent, the North American boreal forest encompasses ~3.7 million km² of which ~58% is classified as forest and other wooded land (Brandt 2009). The North American boreal forest provides ecosystem services at local, regional, and global scales, including the storage of large amounts of carbon in living biomass and soils (Kurz et al. 2013). However, this carbon is vulnerable to climate change, and the amounts sequestered vary in response to changes in forest fires (Amiro et al. 2009) and insect epidemics (Kurz et al. 2008). Both ongoing and projected increases in temperature have been reported, with mean annual temperatures across the Canadian boreal zone expected to increase 4 to 5 °C by 2100 (Price et al. 2013). Climate change has the potential to create positive feedbacks through which decreases in forest carbon sequestration lead to increased atmospheric CO_2 concentrations, further exacerbating climate warming (Soja et al. 2007). More frequent and larger wildfires, increased insect infestations, and changing vegetation structure due to melting permafrost are likely consequences of increased temperatures in the boreal forest region (Price et al. 2013). Therefore, it is useful to examine different approaches for monitoring boreal carbon and to explore the development of new monitoring capabilities (Wulder et al. 2013*a*).

The primary operational approach for assessing large-scale forest biomass and carbon stocks in the boreal forest of North America involves combining forest inventory ground plots with growth and yield curves for different land cover types and disturbance frequencies (Stinson et al. 2011). Laser-ranging airborne lidar has the potential to provide supplemental information on aboveground biomass (AGB) density of forests and has been used increasingly as a sampling tool at local to regional scales (Wulder et al. 2012*a*, 2012*b*). This airborne technology is particularly useful in extending AGB measurements into areas where few, if any, ground plots exist, e.g., unmanaged forest regions.

Airborne lidars provide direct measurements of distances between the aircraft and various ground targets. Data processing algorithms calculate both the distance to the ground and the height above the ground of different components of the forest. From these measurements, a number of lidar metrics related to forest height and canopy structure can be derived, which can then be converted into AGB (Nelson et al. 1988). Both profiling and scanning lidars have been used as sampling tools (e.g., Nelson et al. 2012; Gobakken et al. 2012), and various statistical approaches have been developed to estimate both AGB and carbon stocks, as well as their statistical uncertainties (Gregoire et al. 2011; Ståhl et al. 2011). For example, in lidar-assisted model-based sampling, ground plots representative of the entire area of interest are selected. Models are constructed that predict ground-measured biomass as a function of lidar height and canopy density metrics, and then these models are applied to the entire area (Nelson et al. 2012). The error calculations account for the nonrandom, spatially dependent transect data obtained by the lidar (Ene et al. 2013), which is accomplished partially by using the transect as the sampling unit.

Reliable measurements of forest AGB from a spaceborne lidar would be useful because such an instrument could provide repeated global-scale sampling of variables related to forest height from which regional and global biomass could be derived. The first opportunity to explore the utility of a global sample of satellite-based lidar measurements occurred in 2003 when ICESat-1 (Ice Cloud and land Elevation SATellite) was launched with the Geosciences Lidar Altimetry System (GLAS) aboard. Using the GLAS waveform lidar, the ICESat mission's main objective was to measure changes in the mass balance of the polar ice sheets, and it collected ice elevation data from 2003 to 2009. However, GLAS also offered the scientific community the possibility of estimating forest height and AGB, although the sensor was not explicitly designed for this objective. Global tree height maps have been developed (Simard et al. 2011) and Bolton et al. (2013) compared this information with tree height data in Canada and found that discarding GLAS waveforms from steep terrain reduced errors in height estimates.

Boudreau et al. (2008) and Nelson et al. (2009*a*) applied a sampling approach for 1.3 million km² of forest in the province of Quebec that involved three different sampling phases, i.e., ground, airborne, and satellite. The basic approach involved (*i*) building an initial statistical model to link PALS (Portable Airborne Laser System) height measurements to ground plot biomass, (*ii*) building a second model to relate the estimated biomass from the airborne lidar to the height metrics obtained by GLAS for the 1325 GLAS pulses that were flown by the aircraft, and (*iii*) using the GLAS height metrics, slope, and land cover for the ~104 000 quality-filtered GLAS pulses available across the province of Quebec to calculate the AGB and carbon stocks for the province by land cover type.

In 2008 and 2009, we extended the PALS lidar measurements of ground plots and GLAS ground tracks to the rest of Canada and Alaska. Neigh et al. (2013) used these data in an analysis of the aboveground carbon stocks of the entire circumpolar boreal forest by combining the North American data with similar data in Scandinavia (Næsset et al. 2011) and only ground plot and GLAS data in Siberia (Nelson et al. 2009*b*). They were thus able to compare aboveground carbon stocks between the different regions of the circumpolar boreal.

The goal of the current study is to report for the first time on the detailed results for the three-phase sampling of the 3.7 million km² of the North American boreal forest. We extend the work of Neigh et al. (2013) by reporting detailed estimates of the amount, distribution, and uncertainty of the AGB of the different ecoregions and land cover classes within the boreal forest of North America, analyze some of the factors driving the error estimates, compare our AGB estimates with other available estimates in Canada, and offer our perspectives on the future of lidar sample-based approaches for forest biomass estimation.

Materials and methods

Study area

The study area encompasses the boreal forest biome within Canada and Alaska (Fig. 1) and ranges from a minimum latitude of 44.4°N to a maximum of 69.0°N and from longitudes 52.6°W to 165.0°W. Various definitions and maps of the North American boreal forest have appeared in the literature (e.g., Brandt 2009; Olson et al. 2001). The boundaries of the boreal forest used in the current study were based on those proposed by Brandt (2009, see his fig. 22) for Canada. The Brandt (2009) boundaries were established by digitizing and then harmonizing several existing maps. The northern extent of the boreal forest was defined as the northern tree limit, i.e., the taiga–tundra boundary. Consistent with the traditional approach used in North America for defining the boreal forest, we do not include eastern hardwood forests (e.g., areas in which cold-intolerant hardwoods begin to intermingle with cold-tolerant tree species). On the other hand, we decided to include the Canadian Aspen Forests and Parklands ecoregion in our boreal forest area as it is such an important transition zone that is highly vulnerable to climate change (Michaelian et al. 2011) and is generally considered to be in the boreal zone. For Alaska, we applied additional adjustments to the Brandt (2009) map to retain consistency with the World Wildlife Fund (WWF) ecoregions used as the spatial reporting units (see below). We truncated our boreal biome at the northern US – southern Canadian border, which allowed us to more readily report biomass for the boreal forest in Canada. Areal extents of the boreal forests of Canada and Alaska for our study were 3 326 658 km² (90%) and 370 074 km² (10%), respectively.

Fig. 1. WWF ecoregions of the North American boreal forest.

ICESat-GLAS lidar data

Launched on 12 January 2003, the ICESat satellite carried three lasers packaged within the Geoscience Laser Altimetry System (GLAS). GLAS was the first spaceborne lidar instrument developed for continuous global observations of the Earth. The three lasers were deployed sequentially over the life of the satellite (January 2003 to October 2009). For the current study, we used GLAS data acquisitions 3c and 3f, both of which relied on the last of the three lasers. These collections were used because (*i*) they were the most recent acquisitions available when laser power was still high enough for forest applications and (*ii*) these acquisitions were collected during the growing season in June 2005 and 2006, respectively, and therefore avoided possible contamination of the data from either snow cover or leaf-off conditions.

Previous forest inventory studies that used GLAS as a regional sampling tool in Quebec (Nelson et al. 2009*a*; Boudreau et al. 2008) and Siberia (Nelson et al. 2009*b*) used acquisition 2a. This acquisition, collected between 24 September and 17 November 2003, was used in these previous studies because, at the time that the results were compiled, it was the only acquisition available that was acquired under close to leaf-on conditions. In the current study, the more temporally suitable acquisitions 3c and 3f, collected from 8 to 13 June 2005 and from 8 to 26 June 2006, respectively, were used. However, the differences in the GLAS acquisitions used, combined with the differences in the spatial reporting units, prevent us from making useful quantitative comparisons of AGB between the two studies. In the current study, we only used GLAS pulses that were obtained from footprints that had slopes of <20 degrees as determined by the ASTER DEM (Advanced Spaceborne Thermal Emission and Reflection Radiometer Digital Elevation Model). This was based partially on our analyses of slope effects on biomass regressions from our earlier study (Boudreau et al. 2008). Below, we provide more information on the ASTER DEM.

GLAS collected altimetry data using a 1064 nm laser sending pulses at 40 Hz with a ground footprint that varied in size and shape with laser power, although laser power decreased markedly over time. During acquisitions 3c and 3f, the size of the elliptical footprint of the GLAS pulse was nominally ~60 m × ~40 m, and the distance between pulses was 172 m (Neigh et al. 2013). The GLAS sensors collected waveform data on the intensity of the energy returned from a laser pulse, thus providing information on the vertical distribution of canopy structure (Boudreau et al. 2008). In this study, we made use of both a standard GLAS data product (GLA14) provided by the National Snow and Ice Data Center (NSIDC) and extracted our own structural metrics from the raw waveforms (GLA01) data product. GLA14 is the standard laser altimetry product that uses information from the waveforms recorded over vegetated land by fitting up to six Gaussian distributions to the waveform to describe different features of the vertical structure of the vegetation. The raw GLA01 waveforms were used to calculate additional forest canopy metrics related to forest height and canopy density such as median, mean, and quadratic-mean canopy height, height of different levels of energy return, descriptors of the waveform such as total waveform energy, and various parameters describing the shape of the waveform (Margolis et al. 2015).

Airborne PALS lidar data

PALS is an airborne profiling single-return laser operating at 905 nm that toggles sequentially between first- and last-return laser pulses at rates up to 2 kHz (Nelson et al. 2003*a*). In this study, profiling returns were down-sampled 5:1, i.e., distance measure-

Fig. 2. The locations where ground inventory plots were sampled from the aircraft using the portable airborne lidar system (PALS). The size of the circle indicates the number of ground plots sampled. The solid lines indicate the locations of the GLAS acquisitions 3c and 3f ground tracks that were sampled from the aircraft using PALS. Dark shading indicates the boreal forest.

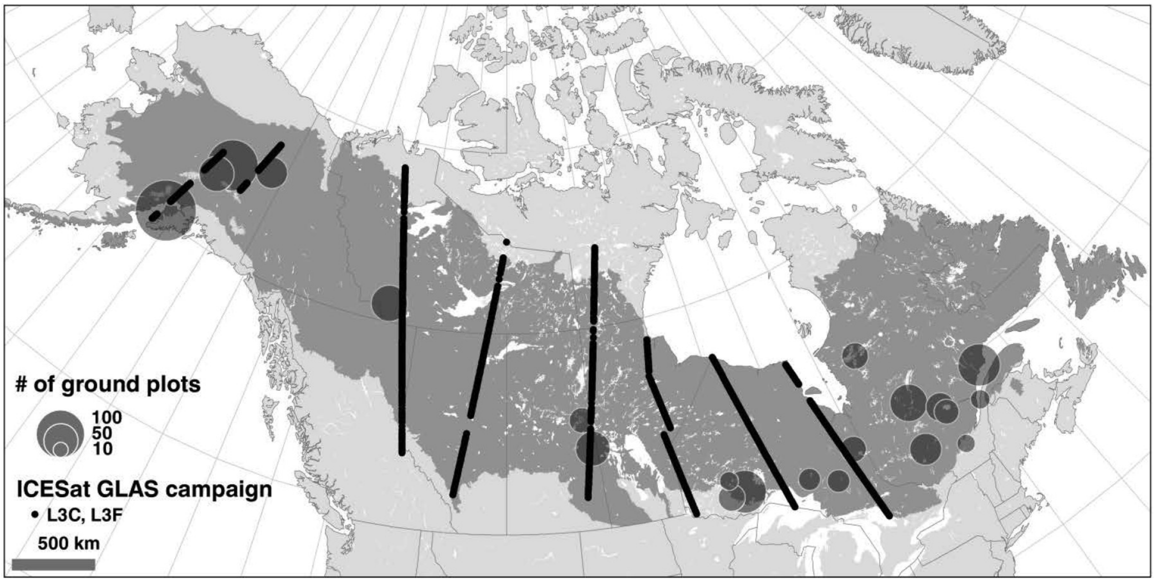

ments from every fifth pulse were recorded, providing an effective ranging rate of 400 Hz. In the postprocessing phase, adjacent first and last returns are combined to derive a first- and last-return data product at 200 Hz.

At an altitude of 150 to 200 m above ground level, the laser illuminates a spot on the ground ~0.4 m in diameter. At a nominal flight speed of 56 m·s^{-1}, sequential 0.4 m footprints were spaced ~0.30 m apart along the track. Postflight processing was done to identify ground returns. A spline was fit to the ground points to define a ground line from the last-return data. Once the ground line was identified, a canopy height could be calculated for each first-return pulse. Thus, the PALS data stream contains information that can be used to calculate canopy height, canopy height variation, and canopy closure.

The PALS sampling only measures forest structure along linear transects of a width defined by the footprint diameter. PALS has successfully collected data for forest inventory analyses (e.g., Nelson et al. 2012) and wildlife habitat evaluation (Nelson et al. 2003*b*, 2005). It was also successfully used as an intermediate sampling tool to tie ground plots to GLAS measurements for a GLAS-based inventory of forest biomass in Quebec (Boudreau et al. 2008; Nelson et al. 2009*a*).

PALS was deployed three times to obtain the data used in the current study: (*i*) in Quebec; (*ii*) in central and western Canada; and (*iii*) in Alaska. The airborne missions were conducted from 31 July to 13 August 2005 in Quebec, from 15 to 27 June 2008 in Alaska, and from 2 July to 7 August 2009 in Canada to the west of Quebec. For Quebec, PALS was mounted on the landing strut of a for-hire Cessna 182. In Alaska, PALS was mounted on the entry–egress step of a Cessna 185 operated by Lighthawk (Lander, Wyoming), a non-profit, environmental aviation organization. For Canada to the west of Quebec, PALS was mounted in the space allocated for the co-pilot inside a for-hire Piper Cherokee PA-32-300 six-seat aircraft. In this case, PALS was installed on a metal mounting rack and viewed the ground through a pre-existing hole cut into the fuselage.

PALS provided measurements for the second, or intermediate, phase of a three-phase sampling design that allowed us to statistically link the forest inventory ground plots to the GLAS footprints. PALS data were obtained over both previously measured geolocated ground plots and were also collected along all of the GLAS 3c and 3f orbital ground tracks used in this study (Fig. 2). Following quality filtering of the GLAS pulses for implausible (e.g., >50 m) height metrics, we had 10 421 coincident PALS–GLAS observations that we used to relate PALS-based estimates of biomass to GLAS measurements. Once these AGB models were in place, we could use GLAS as our regional sampling tool to inventory the North American boreal forest.

Ground inventory plots

The Canadian Forest Service (CFS) worked with various provincial and territorial natural resource management agencies to provide us access to geolocated ground plots within Canada's boreal ecoregions. The inventory plot measurements used in this study were collected in the Northwest Territories (2006–2008), Saskatchewan (2004–2006), Ontario (2006–2007), and Quebec (2001–2004) (Table 1). Consequently, these plot data originated from a number of different jurisdictions (Table 1). The CFS has developed species-specific, national-level equations (Lambert et al. 2005) that we used in this study to convert ground plot measurements of tree height and diameter to AGB. In Alaska, ground plot information was provided by the Forest Inventory and Assessment (FIA) Program of the USDA Forest Service (Woudenberg et al. 2010).

We successfully sampled precisely 1000 geolocated forest inventory sample plots across eastern Canada, western Canada, and Alaska (Table 1) of which 303 were located in Quebec, 196 in Ontario, 80 in Saskatchewan, 57 in the Northwest Territories, and 364 in Alaska (Table 1).

Landsat-derived land cover data

Land cover classifications derived from Landsat data were used for stratification and reporting of AGB by forest stratum. In Canada, we used the 25 m resolution, 23-class EOSD (Earth Observation for Sustainable Development) land cover map of Canada (Wulder et al. 2003, 2013*b*). For Alaska, we used the NLCD-2001 version 1.0 land cover product developed for Alaska at 30 m spatial resolution (http://alaska.usgs.gov/science/geography/nlcd.html). This NLCD product uses 20 land cover classes, but only four of these are forest classes (deciduous forest, conifer forest, mixed forest, treed wetland). We condensed and harmonized the two land cover classifications into the four NLCD forest classes (trees > 5 m) to obtain a

Table 1. The number and location of ground plots by province and ecoregion used to develop the ground plot–PALS equations (total number of plots = 1000).

WWF ecoregions	Province or state	No. of plots	Years of plot measurements	Year of lidar acquisition	Airport base	Latitude (°N)[a]	Longitude (°W)[a]	Data source for plots
Canada (total no. of plots = 636)								
Muskwa–Slave Lake Forests; Northwest Territories Taiga	Northwest Territories	57	2006–2008	2009	Fort Simpson	61.0	123.5	CFS Northern Forestry Centre
Mid-Continental Canadian Forests	Saskatchewan	52	2004–2006	2009	La Ronge	53.4	102.1	Saskatchewan Ministry of Environment
Midwestern Canadian Shield Forests	Saskatchewan	28	2004–2006	2009	La Ronge	55.0	102.8	Saskatchewan Ministry of Environment
Central Canadian Shield Forests	Ontario	78	2006–2007	2009	Thunder Bay	49.1	90.0	Abitibi, Bowater, Buchanan, Domtar
	Ontario	31[b]	2006–2007	2009	Thunder Bay	49.0	91.2	Abitibi, Bowater, Buchanan
	Ontario	15[b]	2006–2007	2009	Dryden	50.0	91.2	Abitibi
	Ontario	21	2006–2007	2009	Marathon	48.7	84.7	Abitibi, Buchanan, Domtar
	Ontario	29	2006–2007	2009	Timmins	49.2	80.4	Abitibi
	Quebec	60	2001–2004	2005	Chibougamau	49.9	74.5	MRNQ
Eastern Canadian Forests	Quebec	35	2001–2004	2005	Roberval	48.8	72.5	MRNQ
	Quebec	77	2001–2004	2005	Baie Comeau	49.4	67.9	MRNQ
	Quebec	16[b]	2001–2004	2005	Rivière du Loup	47.9	69.5	MRNQ
Eastern Forests–Boreal Transition	Quebec	27	2001–2004	2005	Roberval	48.4	72.3	MRNQ
	Quebec	44	2001–2004	2005	Mont Laurier	47.3	75.3	MRNQ
	Quebec	14[b]	2001–2004	2005	Trois-Rivières	46.4	72.4	MRNQ
	Ontario	22	2006–2007	2009	Sudbury	48.0	82.6	Domtar, Abitibi
Eastern Canadian Shield Taiga	Quebec	30	2001–2004	2005	Radisson	53.6	76.4	CFS Laurentian Forestry Centre
Alaska (total no. of plots = 364)								
Cook Inlet Taiga; Copper Plateau Taiga	Alaska	157	2004–2008	2008	Kenai	60.5	151.1	USFS FIA, NPS
Interior Alaska–Yukon Lowland Taiga	Alaska	112	2004–2008	2008	Fairbanks	64.7	147.7	DOD, NPS
Alaska–St. Elias Range Tundra	Alaska	53	2004–2008	2008	Fairbanks	63.8	148.8	NPS, DOD
Interior Yukon–Alaska Alpine Tundra; Oglivie–MacKenzie Alpine Tundra	Alaska	42	2004–2008	2008	Fairbanks	65.5	142.8	NPS

Note: CFS, Canadian Forest Service; MRNQ, Ministère des ressources naturelles du Québec; USFS FIA, United States Forest Service Forest Inventory and Assessment; DOD, US Department of Defense; NPS, US National Park Service.

[a]Approximate geographic center of plot cluster.

[b]Plots located within 75 km of ecoregion boundary.

uniform land cover stratification for all of boreal North America. More specifically, dense, open, and sparse covers in EOSD were harmonized with NLCD covers, respectively, for conifers, hardwoods, mixedwoods, and treed – woody wetland forest covers.

Recently burned areas were overlaid onto the land cover map to provide a unique stratification for this category. Fire polygons from the Canadian Forest Service and the Alaskan Department of Natural Resources were used to define the areas burned between 2001 and 2006, the final year of GLAS acquisitions. Information from the MODIS MCD45 burned area product (Roy et al. 2006) was also used to supplement the fire polygon information when required. Fire is a very common disturbance in the boreal forests of North America, with historical annual burn rates varying from 0.2% to 2.0% across different ecoregions (Bergeron et al. 2004). The burned area biomass values reported in the current article refer only to a subset of the total burned area, i.e., surviving or regenerating forests on areas burned between 2000 and 2006. Furthermore, harvested areas are only included in our analysis if they fell into one of our EOSD or NLCD forest cover classes, e.g., conifer, mixedwood, hardwood, or treed – woody wetland.

Topographic data – ASTER Global Digital Elevation Model and Shuttle Radar Topography Mission

For topographic information at the scale of individual GLAS pulses, we used version 1 of the ASTER Global Digital Elevation Model (GDEM) (http://asterweb.jpl.nasa.gov/gdem.asp). At a spatial resolution of 30 m, the ASTER GDEM has a finer resolution and more northern coverage (83°N) than the Shuttle Radar Topography Mission (SRTM) topographic product that was used for the previous PALS–GLAS analysis in Quebec (60°N, 90 m) (Boudreau et al 2008). We mosaicked the ASTER tiles for each of our three regions (Alaska, western Canada, eastern Canada), masking out

Fig. 3. All of the quality-filtered GLAS orbits for acquisitions 3c and 3f that were used for the regional sampling in this study. Dark shading indicates the boreal forest.

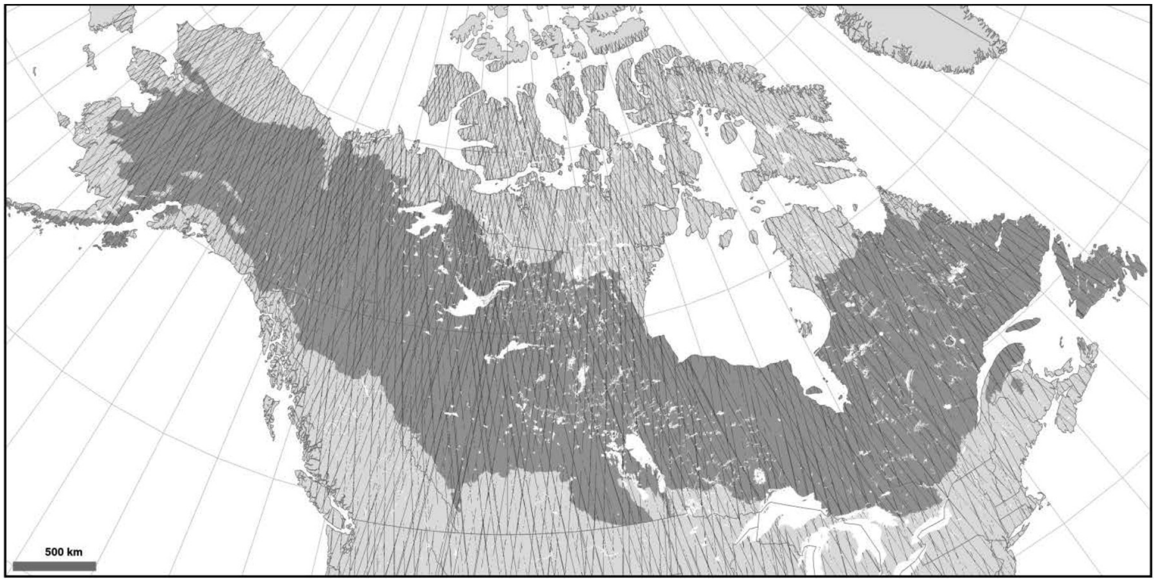

data less than 3 m and more than 6195 m in elevation, the elevation of the highest mountain peak in North America. We then calculated 3 × 3 pixel slopes using the topographic modeling feature in the ENVI 4.1 image process software. For obtaining a general quantification of slopes for different ecoregions to characterize the overall ecoregion topography (e.g., mountainous versus flat, average slope, percentage of forested area per ecoregion above 20° slope), we used a SRTM DEM version at 250 m resolution available from Beaudoin et al. (2014).

Ecoregions

To provide a pan-biome ecosystem-oriented context, we used the WWF map of global terrestrial ecoregions (Olson et al. 2001), which we rasterized to a 1 km resolution. We used this classification to stratify the North American boreal forest into biogeographic reporting units for our AGB estimates. Of the 867 ecoregions identified globally, 22 were located in the North American boreal forest (Fig. 1).

AGB estimation

We used a model-based procedure for estimating AGB density from the ground-plot, PALS, and GLAS data (Nelson et al. 2012; Ståhl et al. 2011). In this procedure, we do not rely on a probability-based forest inventory, rather we use the ground plots that were available and that were as representative as possible of our area of interest, i.e., the plots spanned a wide east to west swath across the North American boreal forest and included plots from both southern and northern portions of the biome (Table 1). In the current case, we applied a three-phase sampling design that linked the three sampling phases (ground plots, airborne profiling lidar, and satellite lidar) via two sets of equations, i.e., a two-phase estimator. The first set of equations estimates ground plot biomass density as a function of the PALS lidar metrics. The second set of predictive equations links the PALS-derived estimates of biomass density, calculated from the first set of equations, to the GLAS metrics. We then used all of the 311 981 quality-filtered GLAS 3c and 3f pulses available in the entire study region (Fig. 3) to obtain AGB estimates for only the forest strata, i.e., conifers, hardwoods, mixedwood, and treed wetlands, where the strata types were determined by the land cover maps. Of the 311 981 quality-filtered GLAS shots, 73.4% of the pulses (229 096 pulses) were identified as measuring one of the four forest strata. Strata identified as nonforest strata, e.g., shrubs, grassland, barren, and urban, were consequently assumed to have zero AGB regardless of the GLAS measurement. Finally, these strata were condensed into the three major regions, i.e., Alaska, western Canada, and eastern Canada.

The estimates of the AGB for a given stratum (land cover, ecoregion, region) from all available GLAS pulses were obtained using eqs. 1 through 4 presented in table 4 of Neigh et al. (2013). Here, we provide a brief summary of the approach. (1) An estimated mean stratum AGB density (in $Mg \cdot ha^{-1}$) for a single ascending or descending ICESat orbit was calculated by averaging the GLAS-based biomass estimates for all pulses intercepting that stratum along an orbit. If a particular stratum was not intercepted along a given orbit, then the stratum mean was taken to be zero. (2) The mean AGB density for a given stratum can then be multiplied by a weighting factor proportional to the area of that stratum within a region or an ecoregion or using eq. 2 from Neigh et al. (2013). (3) The variance of this mean AGB estimate across all strata is provided by eq. 3 in Neigh et al. (2013), and the variance of the individual stratum for AGB density is given in eq. 4 of Neigh et al. (2013). These variance calculations include both sampling error and model error, with the latter term quantifing the variance of the coefficient estimates of the predictive model, i.e., how much the predictive model would change with repeated samples.

In the current context, there is no assumption of randomness in the selection of ground plots. However, there are three other basic assumptions for this model approach. (1) The coincident PALS–GLAS observations are characteristic of the area of interest (AOI, e.g., stratum, ecoregion, or region) and they represent the full range of conditions within the AOI. We note that our decision to exclude GLAS data on >20° slopes violates this assumption to some extent, but we explain why this should not be a major constraint in the Discussion. (2) There is an assumption that the GLAS orbits are randomly acquired. (3) The models to predict biomass for different strata are developed independently.

Estimates of boreal biomass from other sources

We compiled data from two other sources of North American boreal forest AGB to compare with the estimates obtained in our GLAS study. First, we calculated mean AGB density from Canada's National Forest Inventory (NFI) database across the Canadian terrestrial ecozones (Ecological Stratification Working Group 1996) used by NFI for reporting purposes (https://nfi.nfis.org/standardreports.

Table 2. Alaska: summary of linear regressions used for relating ground plot biomass to PALS metrics and PALS biomass to GLAS metrics.

Ecoregion or land cover type	No. of plots or pulses	R^2	RMSE (Mg·ha^{-1})	Independent variables[a]	Largest VIF[b]
Alaska ground plot–PALS equations (by ecoregion, across cover types)					
Cook Inlet Taiga; Copper Plateau Taiga	157	0.60	38.7	hta, h30	2.9
Interior Alaska–Yukon Lowland Taiga	112	0.58	37.9	h95, h10, d60	3.2
Alaska–St. Elias Range Tundra	53	0.80	19.5	h90, h10	1.3
Interior Yukon–Alaska Alpine Tundra; Oglivie–MacKenzie Alpine Tundra	42	0.74	29.2	h70, h40	4.1
Total no. of plots in Alaska	364				
Alaska PALS–GLAS (by cover type, across ecoregions)					
Conifer	345	0.55	20.0	h90, h50, acq	1.9
Hardwood	176	0.53	23.8	h90, h25, acq	1.9
Mixedwood	156	0.54	29.6	qmch, h14, acq	4.9
Wetlands	283	0.56	15.1	h14, h50, fslope, acq	2.0
Burned[c]	179	0.57	17.4	wflen, h90, h25, fslope, acq	6.3
Total no. of GLAS pulses sampled by PALS in Alaska	1139				

Note: Detailed equation parameters are reported in Neigh et al. (2013).

[a]PALS or GLAS independent variables: hta, average height of all returns; h30, height at which 30% of the canopy returns (>1.4 m above ground) have been received (or other percentage of returns, e.g., h90); d60, percentage of returns received from the 60% total height bin whereby each bin is 10% of total canopy height; acq, dummy variable for GLAS acquisition; qmch, quadratic mean canopy height; h14, GLAS14 standard height product; fslope, when the digital number of the lidar return (*x* axis) is plotted against height of the return (or time), fslope is the angle between vertical and the line from signal beginning to the highest peak of the waveform (fslope is related to the canopy roughness, with hardwoods having a high fslope and conifers having a generally lower fslope); wflen, total distance from signal beginning to end.

[b]VIF, variance inflation factor, used to assess co-linearity in the model. A largest VIF value below 10 is considered acceptable.

[c]Because there were no burn observations for the PALS–GLAS sampling, the Alaskan shrub–grass PALS–GLAS equation was used for all ecoregions.

php?lang=en). These calculations use NFI total AGB estimates by forest type, age class, and terrestrial ecozone. The wood volume estimates from the NFI photo plots were then converted by NFI into AGB density using allometric equations and expansion factors (Boudewyn et al. 2007; Stinson et al. 2011).

Unfortunately, standard errors were not tractable at the required forest strata level, so we only had access to mean values. We weighted the respective areas of the WWF ecoregions that fell into each Canadian NFI ecozone. Next, we applied this weighting to the GLAS estimates for each WWF ecoregion to obtain an equivalent GLAS estimate of AGB density for a given Canadian NFI ecozone. In three of the seven cases, the two systems aligned very closely; for the other four cases, there were significant spatial differences between the two systems.

In the second approach, we used 2001 AGB density maps developed at 250 m resolution (i.e., 6.25 ha) using the *k*NN (*k* nearest neighbours) interpolation technique (Beaudoin et al. 2014). This *k*NN approach used the sampling network of NFI photo-plot forest attributes at a maximum sampling rate of 1%, which include AGB as a reference dataset. These AGB estimates are then related to 26 geospatial data layers including 2001 MODIS spectral data, as well as climatic and topographic variables, to expand the NFI estimates to the remaining territory (Beaudoin et al. 2014). Although all forested areas of Canada are included, estimates are generally considered more accurate in the well-inventoried southern NFI ecozones where the NFI photo-plot estimates are more exhaustive and biomass levels are higher (Wulder et al. 2004).

The *k*NN AGB density layer (Mg·ha^{-1}) was used to calculate mean AGB density for each WWF ecoregion (Beaudoin et al. 2014) (Table 13). However, the 250 m *k*NN-based pixels required us to apply a threshold for the percentage of the 10 × 10, 25 m EOSD forested pixels to decide whether or not a given 250 m pixel is considered as forest. We conducted the ecoregion-level calculations using three different threshold values, i.e., 25%, 50%, and 75%. We selected the 75% threshold for estimating *k*NN-based mean AGB density because this threshold provided us with a large number of mostly pure forest pixels and resulted in the closest agreement with GLAS estimates of AGB density. For the GLAS analysis, ecoregion areas were based simply on the number of 25 m resolution (i.e., 0.0625 ha) EOSD forest classes falling within an ecoregion.

Results

Ground plot – PALS relationships

The 1000 forest inventory plots that were sampled by PALS in this study were distributed across 11 of the 22 (50%) WWF boreal forest ecoregions of North America (Table 1; Figs. 1 and 2). Although the plots were largely concentrated in the managed commercial forests of Canada and Alaska, there were also plots in the boreal taiga of northern Quebec and in some fairly remote areas of Alaska (Fig. 2). The plots spanned a large range of AGB densities (range = 0 to 361 Mg·ha^{-1}, mean = 76.3 Mg·ha^{-1}, SD = 58.8; n = 1000) and fell into all four of the major boreal land cover classes (32% conifer, 25% hardwood, 38% mixedwood, and 6% treed wetland). Because this study used a lidar-assisted, model-based sampling approach, we make the assumption that these 1000 plots are representative of our area of interest and therefore meet an important statistical criterion needed to produce an accurate forest inventory.

In Alaska, the most robust regressions for relating PALS metrics to the AGB density of the ground plots were found when we developed equations for specific ecoregions across all forest cover types, with R^2 values ranging from 0.58 to 0.80 (Table 2). In all cases, more than one height metric was selected by the best possible subset regression procedure, typically one variable related to the height of the upper canopy and one or more variables related to the height distribution of laser returns from the lower canopy (Table 2). Throughout the analyses, variance inflation factors (VIF) were monitored and variable selection adjustments were made to keep VIFs well below 10.

In Canada, the most robust ground plot – PALS regressions were found when we developed generic equations for each forest land cover class with all ecoregions pooled, yielding R^2 values ranging from 0.50 to 0.84 (Table 3*a*). For the conifer and treed wetland equations, measurements of both upper and lower canopy

Table 3. Canada: summary of (*a*) generic linear regressions used for relating ground plot biomass to PALS metrics for different land cover types across all ecoregions, i.e., generic equations, and (*b*) linear regressions within specific regions or ecoregions in Canada for which sample size and regression performance were adequate.

(*a*) Ground plot–PALS equations across all ecoregions (generic equations) in Canada

Land cover	No. of plots	R^2	RMSE (Mg·ha^{-1})	Independent variables[a]	Largest VIF[b]
Conifer	184	0.64	32.4	h90, h10	1.2
Hardwood	51	0.65	30.2	h50, d80	1.7
Mixedwood	294	0.50	33.2	qmha, d10	1.3
Wetlands	36	0.84	22.2	h90, hta	5.7
Total no. of plots used for generic equations[c]	565				

(*b*) Ground plot–PALS equations for specific regions or ecoregions in Canada

Region or ecoregion	Land cover type	No. of plots	R^2	RMSE (Mg·ha^{-1})	Independent variables[a]	Largest VIF[b]
Western Canada region[d]	Mixedwood	35	0.64	35.2	htc, d80	1.7
Central Canadian Shield Forests ecoregion	Conifer	60	0.80	22.2	h80, sda	2.2
	Hardwood	41	0.56	26.0	qmch, d80	2.1
	Mixedwood	98	0.60	26.7	h95, d40	1.0
Eastern Forests–Boreal Transition ecoregion	Conifer	29	0.56	37.0	h95, sdc	2.2
	Mixedwood	82	0.48	28.6	hta, d30	1.5
Eastern Canada region[e]	Conifer	66	0.69	27.9	h90, h10	1.8
	Mixedwood	88	0.49	30.8	h40, d80	2.2

Note: Detailed equation parameters are reported in Neigh et al. (2013).

[a]PALS metrics. See Table 2 for definitions. Also: htc, canopy height; sda, standard deviation of total height; sdc, standard deviation of canopy height.

[b]VIF, variance inflation factor, used to assess co-linearity in the model. A largest VIF value below 10 is considered acceptable.

[c]Of the 636 ground plots flown in Canada, 71 plots were not classified as conifer, hardwood, mixedwood, or wetlands by EOSD.

[d]Includes inventory plots located in Muskwa–Slave Lake Forests, Northwest Territories Taiga, Midwestern Canadian Shield Forests, and Mid-Continental Canadian Forests ecoregions.

[e]Includes inventory plots located in the Eastern Canadian Forests and Eastern Canadian Shield Taiga ecoregions.

heights were selected as independent variables, whereas for the hardwood and mixedwood forests, mid- to upper-canopy height measurements paired with canopy density metrics were selected. We were also able to develop robust equations for the major regions of Canada (eastern versus western) and for specific land cover types within some regions and ecoregions (Table 3*b*). These equations had a similar range of R^2 values as the generic equations but slightly lower root mean squared error (RMSE). Therefore, when available, we applied the more specific equations to generate PALS biomass values along the PALS–GLAS flight lines; otherwise, we applied the generic equations for each land cover type.

Our decision to use ecoregion-specific equations across all cover types in Alaska and generic equations for each land cover class across all ecoregions in Canada allowed us to use the equations that yielded the highest R^2 and (or) lowest RMSE values in the different regions and thus should have increased the precision of our estimates. We compared the estimates from these two different stratification approaches across the three main geographic regions and found that the impacts on mean biomass density were on the order of 3% to 5% with no consistent trends, i.e., stratified equations yielded both higher and lower mean AGB density than the nonstratified equations depending on the region. As well, standard errors were similar.

PALS–GLAS relationships

The GLAS 3c and 3f lines that we flew with PALS spanned a large portion of the North American boreal forest in the western and central portions of the biome but did not include much sampling in the eastern portion of eastern Canada (Fig. 2). See the Materials and methods section for reasons why GLAS 2a data from Quebec were not included.

For Alaska, the R^2 values for the regressions relating GLAS metrics to PALS-calculated AGB for each of the five cover types across all ecoregions were very similar and ranged from 0.53 to 0.57 (Table 2). RMSE values were lower than for the ground plot – PALS equations. The conifer and hardwood equations both included a GLAS-derived measurement of upper and lower canopy heights, as well as the GLAS acquisition as a dummy variable (Table 2). For the treed wetlands and burned areas, the GLAS-derived fslope measurement that is related to canopy closure was selected as an independent variable in addition to the height metrics. The fslope variable describes the angle formed between a vertical base line and the leading edge of the waveform; larger angles connote a denser upper canopy layer (see fig. 1 in Boudreau et al. 2008). The mixedwood and burned area equations had higher co-linearity but were still within acceptable ranges (Table 2). We had no coincident measurements of PALS and GLAS for burned areas in Alaska, but we did have 179 data points where PALS flew over GLAS pulses classified as shrubland or grassland (Table 2). Consequently, we applied these shrub–grassland equations to the burned areas in Alaska and used the resulting equation for scaling GLAS to the region for the burned area land cover type (see next section). This is not the ideal method for estimating burned area biomass as GLAS has low sensitivity for detecting vegetation heights less than 5 m (Nelson 2010); however, it does at least provide a quantitative estimate for comparison with future estimates derived using other methods.

For Canada, we developed another set of generic regressions between GLAS metrics and PALS-derived AGB for each forest cover type by region, i.e., western versus eastern Canada (Table 4). However, we did not have a sufficient number of coincident PALS–GLAS observations in burned areas in eastern Canada, so we used the 31 observations available in western Canada to develop an equation that could be applied to burned areas across the country. RMSE values were generally similar to those for the Alaska equations for the three most common forest cover types (conifer, hardwood, mixedwood), ranging from 21.3 to 27.6 Mg·ha^{-1} (Tables 2 and 4). Both R^2 values and sample sizes were higher for the Canadian equations than for Alaska equations, with the exception of

Table 4. Summary of linear regressions used for relating PALS biomass to GLAS metrics for Canada.

Land cover	No. of pulses flown	R^2	RMSE (Mg·ha^{-1})	Independent variables[a]	Largest VIF[b]
PALS–GLAS for western Canada[c]					
Conifer	3042	0.68	21.3	h14, h25	1.4
Hardwood	779	0.63	27.6	wflen, qmhc, acq	3.1
Mixedwood	570	0.59	23.4	qmch, h14, h25	3.5
Wetlands	1567	0.52	27.2	h14, h50, acq	1.9
PALS–GLAS for central and eastern Canada					
Conifer	850	0.62	23.6	h14, h90, h25	4.7
Hardwood	96	0.79	26.4	qmch, h90, h25	3.9
Mixedwood	999	0.70	21.5	h14, senergy, h25	2.0
Wetlands	1348	0.76	9.9	h14, fslope	1.4
PALS–GLAS for all of Canada					
Burn[d]	31	0.66	27.2	qmch, ht-gradj, acq	1.5
Total no. of GLAS pulses sampled by PALS in Canada	9282				

Note: Detailed equation parameters are reported in Neigh et al. (2013).

[a]GLAS metrics. See Tables 2 and 3 for variable definitions. Also: qmch, quadratic mean height of canopy; ht-gradj, distance to ground peak that accounts for the possible presence of two peaks near the ground; senergy, energy returned from the ground peak.

[b]VIF, variance inflation factor, used to assess co-linearity in the model. A largest VIF value below 10 is considered acceptable.

[c]Western Canada is considered as all GLAS lines sampled to the west of the Central Canadian Shield Forests and Southern Hudson Bay Taiga ecoregions.

[d]Due to low sample size, the same PALS–GLAS equation was applied to all 2001–2006 burns in Canada.

treed wetlands in western Canada (Tables 2 and 4). The highest R^2 (0.79) was obtained for hardwood forests in eastern Canada. The GLAS-14 standard height product was selected as an independent variable for six of the nine equations. As found for Alaska, GLAS-derived measurements of both upper and lower canopy heights were included in the equations. The fslope variable describing the density of the upper canopy was selected as an independent variable for treed wetlands in eastern Canada, as it was in Alaska. Co-linearity between independent variables was again at acceptable levels for all PALS–GLAS equations in Canada.

Biomass estimates, distributions, and uncertainties

We present our AGB estimates for each of the three main boreal regions, i.e., Alaska, western Canada, and eastern Canada, and then report our totals for all of North America. Note that we report average biomass densities for the forest areas of the different ecoregions. On the other hand, Neigh et al. (2013) reported biomass densities averaged across forested and nonforested areas of an ecoregion assuming zero biomass for nonforested areas.

Alaska

An individual GLAS orbit is the sampling unit used for estimating AGB at the ecoregion level. In Alaska, there were 57 GLAS 3c and 3f orbits available, which included 22 682 GLAS pulses (Table 5). The number of GLAS orbits available per ecoregion varied from 7 to 55, and the number of GLAS pulses per ecoregion ranged from 29 to 17 025 (Table 5). The Interior Alaska–Yukon Lowland Taiga ecoregion was intercepted by the largest number of orbits (i.e., 55), due in large measure to the very large east–west extent of the ecoregion. The three ecoregions for Alaska with the lowest sampling intensity had only 7 to 8 GLAS orbits each. These three ecoregions also tended to have only small areas occupied by forest. The Alaska–St. Elias Range Tundra ecoregion also supports limited forested areas, but because it is oriented largely in an east–west direction, it was sampled more intensively (29 orbits).

Total AGB for Alaska forests was estimated at 2110 ± 45 Mt (Table 5). The forests of the Interior Alaska–Yukon Lowland Taiga ecoregion contained nearly two-thirds (1386 ± 28 Mt) of the AGB. However, this was due to its large surface area and not to a particularly high AGB density. The forests within the Interior Yukon–Alaska Alpine Tundra ecoregion had the second greatest amount of AGB (15.2%; 320.5 ± 7.4 Mt). These two ecoregions, which accounted for >80% of the total AGB in Alaska, had similar AGB densities (56.3 and 56.9 Mg·ha^{-1}), and these densities were very close to the average for all ecoregions (57.0 ± 1.2 Mg·ha^{-1}).

Model error was a large component of the overall error for all ecoregions (Table 5). The two ecoregions with the greatest number of GLAS orbits also had the highest percent model error (54.4% and 51.0%). The general empirical relationship between the number of orbits, percent model error, and percent sampling error is addressed later.

Conifers were the most intensively sampled stratum (12 547 GLAS pulses), had the largest forest area, and were estimated to contain 54.9% (1159 ± 27.4 Mt) of Alaska's boreal forest AGB. The high sampling intensity for conifers was associated with low sampling error and higher percent model error (80.8%; Table 6). Hardwoods and mixedwoods accounted for similar percentages of the AGB in Alaska (20.5% and 16.4%, respectively), whereas treed wetlands and burned areas were minor components. For AGB density (Mg·ha^{-1}), the hardwood and mixedwood cover types were highest, conifers were intermediate, and treed wetlands and burned areas were lowest (Table 6). Note that burned area in this context refers to surviving or regenerating forests on areas burned between 2000 and 2006.

Western Canada

In western Canada, there were 127 GLAS 3c and 3f orbits available, which included 123 889 GLAS pulses (Table 7). The number of GLAS orbits per ecoregion ranged from 3 (Alaska–St. Elias Range Tundra ecoregion) to 57 (Northern Canadian Shield Taiga ecoregion).

Total AGB for western Canada was estimated at 10 169 ± 170 Mt (Table 7). Over one-third of this AGB was located in the Midwestern Canadian Shield Forests and the Mid-Continental Canadian Forests ecoregions and these ecoregions also had the largest surface areas. Northern Cordillera Forests, Muskwa–Slave Lake Forests, and Canadian Aspen Forests and Parklands accounted for nearly another third of the AGB.

AGB density for western Canada averaged 57.1 (±1.0) Mg·ha^{-1} (Table 7). The lowest AGB density was in the Northwest Territories Taiga (37.6 ± 1.2 Mg·ha^{-1}), and the highest was in the Northern

Table 5. For the Alaskan boreal forest, ecoregion-level estimates of mean aboveground biomass (AGB, dry) density, number of GLAS orbits (flight lines), number of GLAS pulses (observations), model-based standard errors of the estimates, percentage of overall error due to the PALS–GLAS model for each ecoregion, ecoregion area, and total ecoregion AGB, standard error and relative error of total AGB estimate, and percentage of total AGB in each ecoregion.

Ecoregion	Mean AGB (Mg·ha−1)	No. of orbits	No. of pulses	MB SE[a] (Mg·ha−1)	Model error[b] (%)	Ecoregion area in forest (km2)	Total AGB in forest (Mt)	MB SE of total AGB (Mt) (relative error, %)	Total AGB in ecoregion (%)
Alaska Peninsula Montane Taiga	75.5	12	29	10.6	7.7	2602	19.6	2.7 (13.8)	0.9
Cook Inlet Taiga	66.2	8	1 505	4.7	26.3	20 383	134.9	9.7 (7.2)	6.4
Copper Plateau Taiga	49.3	8	1 182	3.2	14.8	14 681	72.4	4.6 (6.4)	3.4
Interior Alaska–Yukon Lowland Taiga	56.3	55	17 025	1.2	51.0	246 085	1385.7	28.5 (2.1)	65.7
Alaska–St. Elias Range Tundra	58.3	29	813	2.4	24.9	21 800	127.2	5.1 (4.0)	6.0
Interior Yukon–Alaska Alpine Tundra	56.9	41	1 694	1.3	54.4	56 335	320.5	7.4 (2.3)	15.2
Ogilvie–MacKenzie Alpine Tundra	60.6	7	434	1.8	24.9	8 188	49.6	1.5 (3.0)	2.4
Average	57.0			1.2	51.9				
Total		57	22 682			370 074	2109.8	44.6 (2.1)	100

[a]MB SE, model-based standard errors for flight lines (orbits) calculated according to the model-based estimator described in Ståhl et al. (2011) and in the Materials and methods section of this article. This error term includes both sampling error due to a limited number of orbits and model error due to error in the PALS–GLAS biomass model.

[b]Model error (%), percentage of the model-based standard error due only to error in the PALS–GLAS biomass model.

Table 6. For the Alaskan boreal forest, stratum-level estimates of mean aboveground biomass (AGB, dry) density, number of GLAS orbits (flight lines),[a] number of GLAS pulses (observations), model-based standard errors of the estimates, percentage of overall error due to the PALS–GLAS model for each stratum, stratum area, total stratum AGB, standard error and relative error of the total AGB estimate, and percentage of total AGB for each stratum.

Land cover stratum	Mean AGB (Mg·ha−1)	No. of pulses	MB SE[b] (Mg·ha−1)	Model error[c] (%)	Stratum area (km2)	Total AGB in stratum (Mt)	MB SE of total AGB (Mt) (relative error, %)	Total AGB in stratum (%)
Hardwood	87.4	2 710	2.6	50.1	49 463	432.3	13.0 (3.0)	20.5
Conifer	56.3	12 547	1.3	80.8	205 900	1159.1	27.4 (2.4)	54.9
Mixedwood	75.7	2 630	4.4	56.8	45 790	346.5	20.2 (5.8)	16.4
Wetland	23.6	4 174	2.1	66.9	58 690	138.6	12.4 (8.9)	6.6
Burned (2000–2006)	32.5	621	2.6	45.6	10 232	33.3	2.7 (8.1)	1.6
Average	57.0		1.2	51.9				
Total		22 682			370 074	2109.8	44.6 (2.1)	100

[a]Number of GLAS orbits (flight lines) = 57.

[b]MB SE, model-based standard errors for flight lines (orbits) calculated according to the model-based estimator described in Ståhl et al. (2011) and in the Materials and methods section of this article. This error term includes both sampling error due to a limited number of orbits and model error due to error in the PALS–GLAS biomass model.

[c]Model error (%), percentage of the model-based standard error due only to error in the PALS–GLAS biomass model.

Cordillera Forests (85.1 ± 2.8 Mg ha−1). Alberta–British Columbia Foothills Forest and Yukon Interior Dry Forests also had high levels of AGB density (81.4 ± 2.5 and 77.8 ± 3.8 Mg·ha−1).

Similar to Alaska, the hardwood cover type in western Canada had the highest AGB density (90.0 ± 1.8 Mg·ha−1), followed by mixedwoods (80.3 ± 1.9 Mg·ha−1; Table 8). Nevertheless, conifers were the largest cover type in the region and therefore held the majority of the total AGB for the region (53.2%), with hardwoods and treed wetlands tied for second place at 16.2% each. Areas burned between 2000 and 2006 were minor contributors to regional AGB (1.5%). The percentage of the error due to the PALS–GLAS model was highest for conifers (52.4%) and burned areas (83.8%); the error for the other cover types was limited more by sampling error.

Eastern Canada

There were 98 GLAS 3c and 3f orbits available in eastern Canada and these included 82 515 pulses (Table 9). The number of GLAS orbits per ecozone ranged from six (Newfoundland Highland Forests) to 49 (Eastern Canadian Shield Taiga).

Total AGB for eastern Canada was estimated at 9554 (±367) Mt (Table 9). More than 77% of the AGB was contained within three ecozones (Eastern Forest–Boreal Transition, Central Canadian Shield Forests, Eastern Canadian Forests). As found for the high AGB ecoregions in the other two regions, these two ecoregions were also among the largest in terms of surface area. Although the Eastern Canadian Shield Taiga and the Southern Hudson Bay Taiga ecoregions also had large surface areas, they only contained 13.4% and 8.2% of the region's AGB, respectively. The relative error for the AGB estimates of the small Newfoundland Highland Forest ecoregion (26.6%) was much higher than for the other ecoregions (3.2% to 8.7%). The percentage of the error due to the PALS–GLAS model varied widely among the ecoregions (11.5%–87.4%) (Table 9).

AGB density was much greater (105.6 ± 3.5 Mg·ha−1) in the Eastern Forest–Boreal Transition ecoregion than in the other ecoregions (Table 9). The two other large forest ecoregions (Central Canadian Shield Forests and Eastern Canadian Forests) had similar AGB densities (68.4 and 67.9 Mg·ha−1). The Southern Hudson Bay Taiga held the lowest AGB density (26.1 Mg·ha−1).

Table 7. For the western Canadian boreal forest, ecoregion-level estimates of mean aboveground biomass (AGB, dry) density, number of GLAS orbits (flight lines), number of GLAS pulses (observations), model-based standard errors of estimates, percentage of overall error due to the PALS–GLAS model for each ecoregion, ecoregion area, total ecoregion AGB, standard error and relative error of total AGB estimate, and percentage of total AGB in each ecoregion.

Ecoregion	Mean AGB (Mg·ha−1)	No. of orbits	No. of pulses	MB SE[a] (Mg·ha−1)	Model error[b] (%)	Ecoregion area in forest[c] (km2)	Total AGB in forest (Mt)	MB SE of total AGB (Mt) (relative error, %)	Total AGB in ecoregion (%)
Alberta–British Columbia Foothills Forest	81.4	20	4 509	2.5	7.8	83 830	682.3	21.2 (3.1)	6.7
Interior Alaska–Yukon Lowland Taiga	41.0	13	1 037	2.1	33.1	13 015	53.4	2.7 (5.1)	0.5
Mid-Continental Canadian Forests	64.0	39	21 909	1.2	17.0	268 798	1 720.6	32.7 (1.9)	16.9
Midwestern Canadian Shield Forests	56.4	49	26 734	1.6	14.4	365 426	2 060.8	58.1 (2.8)	20.3
Muskwa–Slave Lake Forests	53.3	35	13 762	2.2	6.2	200 656	1 069.1	44.1 (4.1)	10.5
Northern Canadian Shield Taiga	38.1	57	23 686	1.1	27.0	254 026	966.9	27.6 (2.9)	9.5
Northern Cordillera Forests	85.1	35	4 461	2.8	13.8	131 722	1 121.1	37.4 (3.3)	11.0
Northwest Territories Taiga	37.6	51	16 564	1.2	26.9	179 746	675.7	22.1 (4.9)	6.6
Yukon Interior Dry Forests	77.8	15	1 537	3.8	7.8	31 367	244.2	12.0 (3.1)	2.4
Canadian Aspen Forests and Parklands	64.4	47	5 415	2.0	7.0	157 325	1 013.0	31.5 (3.1)	10.0
Alaska–St. Elias Range Tundra	55.4	3	45	5.9	2.1	1 183	6.6	0.7 (10.6)	0.1
Interior Yukon–Alaska Alpine Tundra	63.2	32	2 222	2.5	13.7	47 252	298.8	11.8 (3.9)	2.9
Ogilvie–MacKenzie Alpine Tundra	56.8	40	2 008	2.7	11.3	45 237	256.8	12.1 (4.7)	2.5
Average	57.1			1.0	36.2				
Total		127	123 889			1 779 590	10 169.3	170 (1.7)	100

[a]MB SE, standard errors for flight lines (orbits) calculated according to the model-based estimator described in Ståhl et al. (2011) and in the Materials and methods section of this article. This error term includes both sampling error due to a limited number of orbits and model error due to error in the PALS–GLAS biomass model.
[b]Model error (%), percentage of the model-based standard error due only to error in the PALS–GLAS biomass model.
[c]Sum of the forested area falling within each ecoregion as determined by EOSD land cover class, i.e., shrub and nonforested areas are not included.

Table 8. For the western Canadian boreal forest, stratum-level estimates of mean aboveground biomass (AGB, dry) density, number of GLAS orbits (flight lines),[a] number of GLAS pulses (observations), model-based standard errors of estimates, percentage of overall error due to the PALS–GLAS model for each stratum, stratum area, total stratum AGB, standard error and relative error of the total AGB estimate, and the percentage of AGB for each stratum.

Land cover stratum	Mean AGB (Mg·ha−1)	No. of pulses	MB SE[b] (Mg·ha−1)	Model error[c] (%)	Stratum area (km2)	Total AGB in stratum (Mt)	MB SE of total AGB (Mt) (relative error, %)	Total AGB in stratum (%)
Hardwood	90.0	13 300	1.8	31.9	182 902	1 645.6	33.4 (2.0)	16.2
Conifer	58.8	69 369	1.4	52.4	921 245	5 414.6	129.3 (2.4)	53.2
Mixedwood	80.3	11 122	1.9	29.3	163 723	1 314.1	30.5 (2.3)	12.9
Wetland	34.2	28 114	0.9	36.9	480 664	1 644.9	45.6 (2.8)	16.2
Burned (2000–2006)	48.3	1 984	6.3	83.8	31 056	152.3	19.7 (12.9)	1.5
Average	57.1		1.0	36.2				
Total		123 889			1 779 590	10 169.3	170 (1.7)	100

[a]Number of GLAS orbits (flight lines) = 127.
[b]MB SE, standard errors for flight lines (orbits) calculated according to the model-based estimator described in Ståhl et al. (2011) and in the Materials and methods section of this article. This error term includes both sampling error due to a limited number of orbits and model error due to error in the PALS–GLAS biomass model.
[c]Model error (%), percentage of the model-based standard error due only to error in the PALS–GLAS biomass model.

As for the two other boreal regions, conifer forest was the largest land cover type in eastern Canada by more than a factor of two (Table 10), followed by mixedwood and treed wetlands. Conifers contained 4 623.0 (±328.0) Mt of AGB, 48.4% of the total for eastern Canada. Mixedwoods were in second place with 32.8% of the regional AGB. Hardwoods had the highest AGB density (113.6 ± 4.1 Mg·ha−1), followed by mixedwoods (Table 10). Treed wetlands had the lowest AGB density (23.6 ± 1.3 Mg·ha−1). The percentage of the error attributed to the PALS–GLAS model was highest for the conifer and hardwood land covers (87.0% and 72.5%, respectively) and least for treed wetlands (4.5%).

North American boreal forest

We estimate the total AGB of the boreal forest of North America to be 21 836 ± 407 Mt with a relative error of 1.9% (Table 11). This estimate was derived from 256 GLAS orbits containing 229 086 GLAS pulses over a sampling domain of 3.7 million km2. The greatest percentage of this AGB was located in western Canada (46.6%), followed closely by eastern Canada (43.7%). Alaska, which accounted for 10% of the land surface, contained 9.7% of the AGB.

The general distribution of AGB across the boreal forest of North America (Fig. 4) shows the expected latitudinal gradient, with particularly high AGB levels in southern Quebec and southern Ontario. Absolute model-based standard errors were higher in areas with higher AGB, but relative errors were sometimes high both in areas with low AGB, e.g., Southern Hudson Bay Taiga, and in areas with higher AGB, e.g., the Atlantic Provinces (Fig. 4). These maps were compiled by applying an equation for each stratum, where each stratum was a unique combination of land cover class

Table 9. For the eastern Canadian boreal forest, ecoregion-level estimates of mean aboveground biomass (AGB, dry) density, number of GLAS orbits (flight lines), number of GLAS pulses (observations), model-based standard errors of the estimates, percentage of overall error due to the PALS–GLAS model for each ecoregion, ecoregion area, and total ecoregion AGB, standard error and relative error of total AGB estimate, and percentage of total ABG in each ecoregion.

Ecoregion	Mean AGB (Mg·ha−1)	No. of orbits	No. of pulses	MB SE[a] (Mg·ha−1)	Model error[b] (%)	Ecoregion area in forest[c] (km2)	Total AGB in forest (Mt)	MB SE of Total AGB (Mt) (relative error, %)	Total AGB (%)
Eastern Forest–Boreal Transition	105.6	30	11 331	3.5	50.9	259 832	2 743.2	89.1 (3.2)	28.7
Central Canadian Shield Forests	68.4	48	21 196	2.4	52.4	334 425	2 288.5	81.0 (3.5)	24.0
Eastern Canadian Forests	67.9	42	12 926	4.1	87.4	352 672	2 393.4	145.2 (6.1)	25.1
Eastern Canadian Shield Taiga	44.5	49	13 762	3.9	41.2	288 493	1 284.7	111.8 (8.7)	13.4
Newfoundland Highland Forests	56.0	6	329	14.9	11.5	10 600	59.4	15.8 (26.6)	0.6
Southern Hudson Bay Taiga	26.1	48	22 971	1.6	12.1	301 045	784.6	48.8 (6.2)	8.2
Average	61.8			2.4	70.3				
Total		98	82 515			1 547 068	9 553.8	367.1 (3.8)	100

[a]MB SE, standard errors for flight lines (orbits) calculated according to the model-based estimator described in Ståhl et al. (2011) and in the Materials and methods section of this article. This error term includes both sampling error due to a limited number of orbits and model error due to error in the PALS–GLAS biomass model.

[b]Model error (%), percentage of the model-based standard error due only to error in the PALS–GLAS biomass model.

[c]Sum of the forested area falling within each ecoregion as determined by EOSD land cover class, i.e., shrub and nonforested areas are not included.

Table 10. For the eastern Canadian boreal forest, stratum-level estimates of mean aboveground biomass (AGB, dry) density, number of GLAS orbits (flight lines),[a] number of GLAS pulses (observations), model-based standard errors of the estimates, percentage of overall error due to the PALS–GLAS model, stratum area, total stratum AGB, standard error and relative error of the total AGB estimate, and the percentage of AGB for each stratum.

Land cover stratum	Mean AGB (Mg·ha−1)	No. of pulses	MB SE[b] (Mg·ha−1)	Model error[c] (%)	Stratum area (km2)	Total AGB in stratum (Mt)	MB SE of total AGB (Mt) (relative error, %)	AGB in stratum (%)
Hardwood	113.6	4 459	4.1	72.5	91 260	1 036.7	37.4 (3.6)	10.8
Conifer	59.2	38 234	4.2	87.0	780 904	4 623.0	328.0 (7.1)	48.4
Mixedwood	85.9	20 368	3.3	8.7	365 047	3 135.8	120.5 (3.8)	32.8
Wetland	23.6	19 029	1.3	4.5	300 164	708.4	39.0 (5.5)	7.4
Burned (2000–2006)	53.1	425	9.9	38.4	9 693	51.5	9.6 (18.6)	0.5
Average	61.8		2.4	70.3				
Total		82 515			1 547 168	9 555.3	367.1 (3.8)	100.0

[a]Number of GLAS orbits (flight lines) = 98.

[b]MB SE, standard errors for flight lines (orbits) calculated according to the model-based estimator described in Ståhl et al. (2011) and in the Materials and methods section of this article. This error term includes both sampling error due to a limited number of orbits and model error due to error in the PALS–GLAS biomass model.

[c]Model error (%), percentage of the model-based standard error due only to error in the PALS–GLAS biomass model.

Table 11. For the North American boreal forest, region- or stratum-level estimates of total aboveground biomass (AGB, dry), model-based standard errors and relative errors of the estimates, number of GLAS orbits (flight lines), number of GLAS pulses (observations), region or stratum forest area, and percentage of total AGB in each region or stratum.

	Total AGB in forest (Mt)	MB SE[a] (Mg·ha−1)	Relative error (%)	No. of orbits	No. of pulses	Boreal forest area (km2)[b]	Total AGB (%)
Region							
Alaska	2 110	45	2.1	57	22 682	370 074	9.7
Western Canada	10 169	170	1.7	127	123 889	1 779 590	46.6
Eastern Canada	9 554	367	3.8	98	82 515	1 547 068	43.7
Total	21 836	407	1.9	256	229 086	3 696 732	100
Land cover stratum							
Hardwood	3 114	52	1.7	256	20 469	323 624	14.3
Conifer	11 196	351	3.1	256	120 420	1 908 048	51.3
Mixedwood	4 797	127	2.6	256	34 120	574 560	22.0
Wetland	2 492	61	2.4	256	51 317	839 518	11.4
Burned (2000–2006)	238	22	9.3	256	3 030	50 980	1.1
Total	21 836	407	1.9	256	229 356	3 696 732	100

[a]MB SE, standard errors for flight lines (orbits) calculated according to the model-based estimator described in Ståhl et al. (2011) and in the Materials and methods section of this article. This error term includes both sampling error due to a limited number of orbits and model error due to error in the PALS–GLAS biomass model.

[b]Sum of the forested area falling within each region or stratum as determined by EOSD land cover class, i.e., shrub and nonforested areas are not included.

and ecoregion. Each stratum-level equation was used to calculate stratum-level AGB density and error values, which were then assigned to each pixel within the stratum. The conifer land cover class accounted for 51% of the AGB and covered 52% of the total forest area. Mixedwood and hardwood forests contained an additional 36% of the biomass and covered about one-quarter of the total forest area (Table 11). Treed wetlands also covered about one-quarter of the forest area but accounted for only 11% of the

Fig. 4. Maps of (top) the distribution of aboveground biomass (AGB) density (Mg·ha⁻¹), (middle) two times the model-based standard error (Mg·ha⁻¹), i.e., the ~95% confidence interval on the strata means, and (bottom) the relative error (%) of the AGB densities, i.e., (SE/mean) × 100. The maps were derived by assigning a mean AGB density class to each land cover class within an ecoregion based on the PALS–GLAS equations in Table 2 (Alaska) and Table 4 (western and eastern Canada).

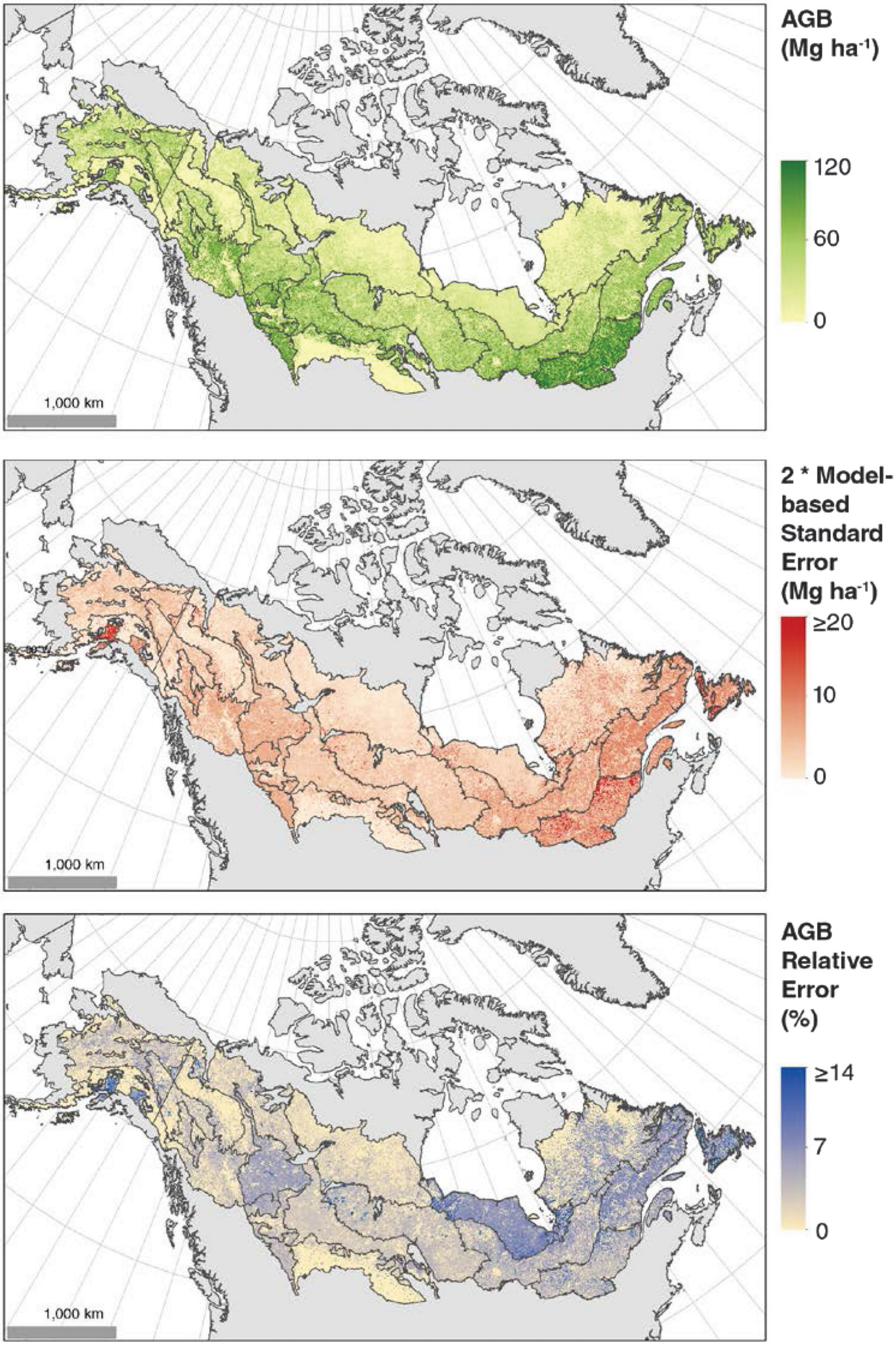

AGB. Recently burned areas were only minor contributors to both AGB and surface area (~1%). The relative errors of the estimates were less than 3.1% for each cover type, except for the burned areas, which had a relative error of 26% (Table 11).

Discussion

Relative contribution of error terms

The relative contribution of model error to the overall error should vary as a function of (*i*) the variability in model coefficients and (*ii*) the number of GLAS orbits that intercept a given ecoregion (Tables 2 and 4). The sampling unit for our AGB estimates is the individual GLAS orbit, e.g., the mean AGB estimated for a given cover type or ecoregion within a given orbit. In this context, we define an orbit as either the ascending or descending portion of a single complete near-polar transit of the Earth. Because GLAS is a north–south near-polar orbiter, small ecoregions that are limited in their east–west extent have fewer GLAS orbits, greater sampling error, and usually a lower percent model error (e.g., Yukon Interior Dry Forests, Copper Plateau Taiga, Cook Inlet Taiga). Modeling error tends to be stable regardless of the size of the area of interest (Nelson et al. 2012) and is not impacted by differences in sampling intensity.

Additional sources of error

In the current study, we did not account for the scatter around the PALS estimate of ground-measured biomass, even though the model errors associated with the ground plot – PALS regressions are large (Table 3). This omission is due to the fact that the statistical methods for rigorously integrating the ground plot – PALS uncertainty into the overall uncertainty do not yet exist. How large is this missing error component? Although we cannot be certain, Neigh et al. (2013) provide some indication of the magnitude. In their circumpolar boreal study, they used a model-dependent, two-phase estimator (Ståhl et al. 2011) to estimate biomass in western Eurasia and, separately, in eastern Eurasia. The Ural Mountains divide these two regions. The two-phase estimator refers to the set of statistical equations that relate two data sources, for instance, airborne lidar data and satellite lidar data. In western Eurasia, Neigh et al. (2013) employed a three-phase sampling approach (ground–air–satellite) with Ståhl et al.'s (2011) two-phase estimator, as we did in the current study. In eastern Eurasia, on the other hand, Neigh et al. (2013) employed only a two-phase sampling approach (ground and satellite sampling), but once again used the same Ståhl et al. (2011) two-phase estimator. Mean AGB density for western Eurasia was 19.4 ± 1.0 Mg·ha^{-1}, whereas for eastern Eurasia, it was 22.7 ± 3.4 Mg·ha^{-1}. The 3.4 times greater standard error for eastern Eurasia suggests that the missing ground to airborne lidar variance term increases standard errors around three- to four-fold. This highlights the need for a model-dependent, three-phase estimator that will link the three sources of data (ground–air–satellite). Such work is being undertaken and progress has been made (Ståhl et al. 2014). However, the limited number of ground plots and the consequent lack of stratification by cover type or ecoregion for these eastern Eurasia estimates are also possible reasons for the higher uncertainty.

The two-phase estimator used in the current study is more stable and robust than the simple random sampling estimator with covariance terms added that was employed in our earlier studies (Nelson et al. 2009*a*). Our current estimator is statistically defensible (Ståhl et al. 2011) and properly accounts for two variance sources, the sampling component (GLAS orbit-to-orbit variation) and the regression component (the variability of the coefficients of the predictive regressions used to calculate estimates of biomass based on satellite measurements). Ene et al. (2013) used a boreal forest sampling simulator to confirm that the Ståhl et al. (2011) estimator is unbiased when random sampling assumptions are met but prone to variance overestimation when there is a systematic sample of airborne lidar flight lines in an area with a marked regional biomass trend across the transects. Ene et al. (2013) demonstrated that inclusion of the successive difference (SD) variance estimator in place of the Ståhl et al. (2011) sampling variance term can significantly mitigate the well-documented variance inflation noted when systematic samples are treated as a random sample. We expect to include the SD estimator in our future North American AGB analyses.

The uncertainty due to the allometry models (Lambert et al. 2005) that were used to calculate plot-level biomass of individual trees from tree diameter and height were also not included in our error analysis. However, McRoberts and Westfall (2014) have demonstrated that the error in the allometric equations is a small source of uncertainty for large area volume estimates in the boreal forest if sample sizes are sufficiently large, i.e., >100 sample trees per species). Nevertheless, how to robustly integrate the error due to allometric equations into large-area biomass estimates is still an open question that requires additional research.

Neigh et al. (2013) discuss other possible sources of error in a three-phase sampling approach (e.g., geolocation errors, land cover misclassification, DEM artifacts). Furthermore, the use of an airborne scanning lidar, rather than a profiling lidar such as we used in the current study, has been shown to reduce the total variance of the estimates due mostly to the improved accuracy of the regression models from scanner data for boreal forests (Ståhl et al. 2011). Therefore, we emphasize that the error estimates that we present only account for sampling error and PALS–GLAS model error and that the true magnitude of the uncertainty in our estimates is likely to be higher.

To determine the implications of applying the 20° slope threshold for excluding GLAS data, we used 250 m composites of SRTM topography and EOSD land cover to calculate the percentage of the total forested area per ecoregion that had slopes above the threshold in Canada. The three steepest ecoregions (Northern Cordillera Forests, Ogilvie–MacKenzie Alpine Tundra, Interior Yukon–Alaska Alpine Tundra) had values of 7.3%, 4.9%, and 2.1%, respectively. All of the other ecoregions were below 2%. We conclude that the impact of our slope filtering was minor in large part because forests are fairly uncommon on slopes steeper than the threshold.

Comparison with other estimates of boreal biomass

The differences between the NFI-based estimates of mean biomass density and our GLAS estimates for Canada were within 17% for those NFI ecozones that were well inventoried by the NFI (Boreal Cordillera, Boreal Shield, Boreal Plains) (Table 12). However, for less intensively sampled northern NFI ecozones, the relative differences between the GLAS and NFI estimates ranged from −24.3% to −44.7%, except for the Hudson Plains ecozone (Table 12). This suggests that the GLAS estimates may better capture the state of AGB in these more remote areas and that both methods otherwise provided similar answers when sufficient NFI photo plots were present. Five of the seven Canadian NFI ecozones did not have a close spatial match to the WWF ecoregions and therefore the weighting of the WWF ecoregion estimates was a potential source of error. Overall, GLAS and NFI estimates of AGB density were within 18.6% (13.6 Mg·ha^{-1}) for the Canadian boreal forest.

When we compared GLAS with the *k*NN estimates of AGB density for the boreal forest of Canada, the relative difference for AGB density was less than 26% (absolute value) for eight of the well-inventoried and three of the less inventoried northern WWF ecoregions (Table 13) representing 67% of the boreal forest area of Canada. In contrast to the NFI comparison, GLAS estimates of total ecoregion AGB were higher for 16 of the 18 WWF ecoregions in Canada. There was a positive correlation between the relative difference of AGB density and the average slope of the terrain across ecoregionss (r = 0.62) and a negative correlation between

Table 12. Comparison between GLAS and direct Canada National Forest Inventory (NFI) estimates of mean aboveground biomass (AGB, dry) density by Canadian boreal ecozone. Shaded part of the table indicates Canadian ecozones well inventoried by the NFI, whereas unshaded part indicates partially or poorly inventoried northern ecozones. Ecozones are sorted by increasing absolute values of relative differences of means for well-inventoried and partially or poorly inventoried ecozones, respectively.

Canadian ecozone	NFI mean AGB density (Mg·ha^{-1})	Equivalent WWF ecoregions	Weighted GLAS mean AGB density (Mg·ha^{-1})	Difference of means (GLAS–NFI) (Mg·ha^{-1})	Relative difference of means (GLAS–NFI)/NFI) (%)
Boreal Cordillera*	71.4	Northern Cordillera Forests + Interior Yukon–Alaska Alpine Tundra (latter only partially overlaps Boreal Cordillera)	79.1	7.7	10.8
Boreal Shield*	81.4	Midwestern Canadian Shield Forests + Central Canadian Shield Forests + Eastern Forest–Boreal Transition + Eastern Canadian Forests	72.3	–9.1	–11.2
Boreal Plains*	79.9	Mid-Continental Canadian forests + Canadian Aspen Forests and Parklands + Alberta–British Columbia Foothills Forests (latter only partially overlaps with Boreal Plains)	66.9	–13.0	–16.3
Hudson Plains	24.4	Southern Hudson Bay Taiga	26.1	1.7	7.0
Taiga Shield	54.8	Eastern Canadian Shield Taiga + Northern Canadian Shield Taiga	41.5	–13.3	–24.3
Taiga Cordillera*	76.7	Ogilvie–MacKenzie Alpine Tundra (smaller than Taiga Cordillera)	56.8	–19.9	–26.0
Taiga Plains*	82.9	Northwest Territories Taiga + Muskwa–Slave Lake Forests (latter has only minor overlap with Taiga Plains)	45.9	–37.0	–44.7
Average for Canadian boreal forest	72.9		59.3	–13.6	–18.6

Note: Asterisk (*) indicates significant differences in geographic matching between the two systems.

slope and mean AGB ($r = -0.78$). Consequently, relative differences were the lowest for flat or gently rolling ecoregions, particularly those with higher AGB densities such as the Central Canadian Shield Forests (0.8%) (Table 13). At the other extreme, relative differences were highest for mountainous ecoregions, particularly for those with low biomass levels located in poorly inventoried northern regions. The worst was for the mountainous Ogilvie–Mackenzie Alpine Tundra ecoregion (62.2%).

For the entire boreal forest of Canada, the discrepancy of 2.2 Mg·ha^{-1} (3.7%) between the AGB densities derived from GLAS versus *k*NN leads to a 0.8 Pg difference in AGB when scaled to the entire 3.7 million km^2 area of the North American boreal forest in the context of a GLAS-based total AGB estimate of 21.8 Pg.

Beaudoin et al. (2014) found that the *k*NN estimates of AGB density were less accurate for mountainous areas, as well as for poorly inventoried northern ecoregions with low AGB density. However, because GLAS is also known to perform poorly in steep topography, we are not able to judge which technique performed best under these conditions. One difference between the two approaches is that we removed GLAS data having >20% slope based on results from a previous study (Boudreau et al. 2008), whereas the *k*NN technique does not include any topographic filtering. As well, in remote areas, the *k*NN technique extrapolates outside the geographical distribution of the NFI photo plots used for training. This suggests that the GLAS estimates of AGB density could be more accurate in poorly inventoried, relatively flat ecoregions.

Pertinence to future spaceborne lidar missions for forest biomass estimation

GLAS was the first spaceborne lidar instrument to be launched that could provide estimates of forest AGB and it indeed succeeded in collecting a valuable dataset over a multiyear period. The VCL (Dubayah et al. 1997) and DESDynI (Hall et al. 2011) satellites were both attempts to develop a spaceborne lidar designed specifically for vegetation structure, but both missions were cancelled. More recently, a proposal to install a vegetation lidar (GEDI, Global Ecosystem Dynamics Investigation) on the International Space Station (ISS) in 2018–2019 has been approved and has now entered an advanced planning stage. However, the orbital limit of the ISS is 50°N–50°S, so GEDI will be of limited utility for monitoring the North American boreal forest. Planning is also underway for the US–India S- and L-band NISAR and the European P-band BIOMASS satellites. Both of these radar satellites have AGB estimation as a central mission objective.

Another opportunity to continue spaceborne lidar remote sensing of forest structure lies with ICESat-2, currently scheduled for launch in 2017. ICESat-2 will use the Advanced Topographic Laser Altimeter System (ATLAS) micropulse, multibeam, photon-counting lidar that has a lower energy, but a higher repetition rate, than the analog waveform system used on ICESat (Herzfeld et al. 2014). A secondary mission objective for ICESat-2 is to provide measurements of vegetation height at a maximum between-adjacent-orbit spacing of <2 km. However, the lower energy and lower signal-to-noise ratio present significant challenges to implementing this technology for estimating forest height and AGB. For example, a preliminary study simulating ICESat-2 returns across modeled *Larix* spp. stands indicates AGB density errors of 20% to 50% for AGB densities above 20 Mg·ha^{-1} (Montesano et al. 2015). A possible advantage of the multibeam, photon-counting approach would be the much greater sampling density, which will greatly increase the probability that existing forest inventory plots are directly measured by the satellite. This could permit a two-stage sampling strategy to be implemented (ground plots and spaceborne lidar) for AGB estimation (Ene et al. 2013) and thus avoid the need for the more elaborate theoretical framework required for three-phase sampling.

Conclusions

We have presented estimates of the amount, distribution, and uncertainty of AGB of the different ecoregions and land cover classes within the boreal forest of North America using a spaceborne lidar, analyzed some of the factors driving the error estimates, and compared our AGB estimates with other available North American estimates. Only sampling error and airborne–spaceborne model error were included in the uncertainty estimates. Our relative errors were generally under 4% for the three

Table 13. Comparison of percent forested areas and aboveground biomass (AGB) densities between GLAS-based and *k*NN-based estimates for WWF ecoregion level estimates in the Canadian boreal forest. Ecoregions are sorted by increasing absolute value of relative difference. Shaded areas indicate well-inventoried ecoregions.

	Mean slopes and percent forested areas				Mean AGB density (Mg·ha^{-1})			
Ecoregion[a]	Mean slope (°)	Forested area, *k*NN at 75% threshold[b] (%)	Forested area, GLAS[c] (%)	Relative difference in percent forested area ((GLAS–*k*NN)/GLAS)	*k*NN[d]	GLAS	Difference (GLAS–*k*NN)	Relative difference ((GLAS–*k*NN)/GLAS) (%)
Canadian Aspen Forests and Parklands	0.8	16.3	39.4	58.6	64.0	64.4	0.4	0.7
Central Canadian Shield Forests	1.1	58.8	72.2	18.6	67.8	68.4	0.6	0.8
Alberta–British Columbia Foothills Forests	2.6	63.7	69.3	8.1	83.7	81.4	–2.3	–2.8
Eastern Canadian Forests	3.6	58.0	72.2	19.7	64.7	67.9	3.2	4.6
Midwestern Canadian Shield Forests	1.0	46.8	66.6	29.7	52.8	56.4	3.6	6.3
Muskwa–Slave Lake Forests	1.2	51.5	76.1	32.3	48.4	53.3	4.9	9.3
Eastern Canadian Shield Taiga	2.2	19.3	38.1	49.3	39.8	44.5	4.7	10.5
Eastern Forest–Boreal Transition	2.7	71.5	74.5	4.0	92.3	105.6	13.3	12.6
Mid-Continental Canadian Forests	0.8	56.7	72.7	22.0	55.5	64.0	8.5	13.4
Newfoundland Highland Forests	3.8	29.1	64.7	55.0	43.6	56.0	12.4	22.1
Northern Cordillera Forests	11.5	42.1	49.9	15.6	63.4	85.1	21.7	25.5
Northern Canadian Shield Taiga	1.0	15.8	41.1	61.6	25.0	38.1	13.1	34.4
Yukon Interior Dry Forests	6.2	38.3	50.0	23.4	46.7	77.8	31.1	39.9
Southern Hudson Bay Taiga	0.3	36.5	80.2	54.5	37.2	26.1	–11.1	–42.4
Northwest Territories Taiga	2.6	30.7	51.6	40.5	21.3	37.6	16.3	43.4
Interior Alaska–Yukon Lowland Taiga	2.8	12.8	42.2	69.7	21.8	41.0	19.2	46.8
Interior Yukon–Alaska Alpine Tundra	8.3	26.2	33.5	21.8	33.4	63.2	29.8	47.2
Ogilvie–MacKenzie Alpine Tundra	13.9	14.1	21.6	34.7	21.5	56.8	35.3	62.2
Average for Canadian boreal forest	3.3	38.7	59.8	35.3	57.1	59.3	2.2	3.7

[a]The Alaska–St. Elias Range Tundra ecoregion was not included as it is only marginally located within Canada.
[b]Percent forested areas within an ecoregion were calculated using a 75% threshold for the percentage of 25 m EOSD forest classes falling within a 250 m *k*NN pixel.
[c]GLAS percent forested area estimates are based directly on whether the 25 m EOSD pixels are classified as forest.
[d]*k*NN biomass density was calculated only for 250 m MODIS pixels having >75% of their 25 m EOSD pixels classified as forest.

regions and for the major cover types in these regions and under 10% for ecoregions. The exception to this was for recently burned areas (9.3% relative error), likely due to the insensitivity of GLAS in short vegetation (Montesano et al. 2014). Ecoregions that are limited in their east–west extent tended to have a greater percent sampling error due to the limited number of GLAS orbits crossing these ecoregions. There are other sources of error that were not explicitly included in the current analysis that should be addressed in future work if statistical theory advances to the point where this becomes tractable, e.g., errors due to the allometric models, to uncertainty in model parameters for the regressions between ground plots and airborne lidar metrics, to geolocation – field measurement errors, to land cover misclassification, and to artifacts in the DEM.

The comparisons of the GLAS AGB estimates for Canada with those derived from National Forest Inventory photo plots and from the *k*NN spectral modelling approach reinforced our confidence in the quality of our GLAS estimates, although differences were generally much greater for more remote northern ecoregions with low AGB densities and for ecoregions with higher relief and more fragmented forested landscapes. GLAS estimates of average AGB density were in close agreement with the *k*NN approach for the entire boreal forest in Canada (absolute difference of 2.2 $Mg \cdot ha^{-1}$, relative difference of 3.7%), although differences were greater for the less inventoried, more remote ecoregions.

Although GLAS stopped obtaining data for forest applications in 2006, our study still provides a useful proof-of-concept of how a spaceborne lidar can be combined with ground plots and airborne measurements to conduct large-scale AGB assessments at the biome scale for both the density and the total AGB. The approach described here provides a framework for making repeated, periodic, satellite-based forest inventories to monitor boreal forest AGB over time.

Acknowledgements

This work was funded by a NASA Carbon Cycle Science grant (NNH07ZDA001N-CARBON) to RFN with an additional contribution for the Canadian portion of the work from an Natural Sciences and Engineering Research Council of Canada (NSERC) Discovery grant to HAM. This work was part of a university sabbatical project of HAM at NASA Goddard. We thank the USRA-GESTAR Program, IMSG Inc., Infrared Baron Inc., Tad Fickel (pilot), Ryan Collins (pilot), Karen Zhou (Ontario Ministry of Natural Resources), and Canadian Forest Service personnel Mark Gillis (National Forest Inventory), Ron Hall (Northern Forestry Centre), and Philippe Villemaire (Laurentian Forestry Laboratory) for their contributions to this study. We also thank all of the US and Canadian agencies at the federal, state, and provincial levels for providing access to ground-plot and photo-plot data. Finally, we gratefully acknowledge the helpful comments from three reviewers and the Associate Editor.

References

Amiro, B.D., Cantin, A., and Flannigan, M.D. 2009. Future emissions from Canadian boreal forest fires. Can. J. For. Res. **39**: 383–395. doi:10.1139/X08-154.

Beaudoin, A., Bernier, P.Y., Guindon, L., Villemaire, P., Guo, X.J., Stinson, G., Bergeron, T., Magnussen, S., and Hall, R.J. 2014. Mapping attributes of Canada's forests at moderate resolution through *k*NN and MODIS imagery. Can. J. For. Res. **44**: 521–532. doi:10.1139/cjfr-2013-0401.

Bergeron, Y., Flannigan, M., Gauthier, S., Leduc, A., and Lefort, P. 2004. Past, current and future fire frequency in the Canadian boreal forest: implications for sustainable forest management. Ambio, **33**: 356–360. doi:10.1579/0044-7447-33.6.356.

Bolton, D.K., Coops, N.C., and Wulder, M.A. 2013. Investigating the agreement between global canopy height maps and airborne lidar derived height estimates over Canada. Can. J. Remote Sens. **39**: S139–S151. doi:10.5589/m13-036.

Boudewyn, P., Song, X., Magnussen, S., and Gillis, M.D. 2007. Model-based, volume-to-biomass conversion for forested and vegetated land in Canada. Natural Resources Canada, Canadian Forest Service, Pacific Forestry Centre, Victoria, B.C., Inf. Rep. BC-X-411.

Boudreau, J., Nelson, R.F., Margolis, H.A., Beaudoin, A., Guindon, L., and Kimes, D.S. 2008. Regional aboveground forest biomass using airborne and spaceborne LiDAR in Quebec. Remote Sens. Environ. **112**: 3876–3890. doi:10.1016/j.rse.2008.06.003.

Brandt, J.P. 2009. The extent of the North American boreal zone. Environ. Rev. **17**: 101–161. doi:10.1139/A09-004.

Dubayah, R., Blair, J.B., Bufton, J.L., Clark, D.B., JaJa, J., Knox, R., Luthcke, S.B., Prince, S., and Weishampel, J. 1997. The vegetation canopy lidar mission. *In* Proceedings of Land Satellite Information in the Next Decade, II: Sources and Applications, Bethesda (MD). American Society of Photogrammetry and Remote Sensing. pp. 100–112.

Ecological Stratification Working Group. 1996. A national ecological framework for Canada. Agriculture and Agri-Food Canada, Research Branch, Centre for Land and Biological Resources Research and Environment Canada, State of the Environment Directorate, Ottawa.

Ene, L.T., Naesset, E., Gobakken, T., Gregoire, T.G., Stahl, G., and Holm, S. 2013. A simulation approach for accuracy assessment of two-phase post-stratified estimation in large-area LiDAR biomass surveys. Remote Sens. Environ. **133**: 210–224. doi:10.1016/j.rse.2013.02.002.

Gobakken, T., Næsset, E., Nelson, R., Bollandsås, O.M., Gregoire, T.G., Ståhl, G., Holm, S., Ørka, H.O., and Astrup, R. 2012. Estimating biomass in Hedmark County, Norway, using national forest inventory field plots and airborne laser scanning. Remote Sens. Environ. **123**: 443–456. doi:10.1016/j.rse.2012.01.025.

Gregoire, T.G., Ståhl, G., Naesset, E., Gobakken, T., Nelson, R., and Holm, S. 2011. Model-assisted estimation of biomass in a LiDAR sample survey in Hedmark County, Norway. Can. J. For. Res. **41**: 83–95. doi:10.1139/X10-195.

Hall, F.G., Bergen, K., Blair, J.B., Dubayah, R., Houghton, R., Hurtt, G., Kellndorfer, J., Lefsky, M., Ranson, J., Saatchi, S., Shugart, H.H., and Wickland, D. 2011. Characterizing 3D vegetation structure from space: mission requirements. Remote Sens. Environ. **115**: 2753–2775. doi:10.1016/j.rse.2011.01.024.

Herzfeld, U.C., McDonald, B.W., Wallin, B.F., Neumann, T.A., Markus, T., Brenner, A., and Field, C. 2014. Algorithm for detection of ground and canopy cover in micropulse photon-counting lidar altimeter data in preparation for the ICESat-2 mission. IEEE Trans. Geosci. Remote Sens. **52**(4): 2109–2125. doi:10.1109/TGRS.2013.2258350.

Kurz, W.A., Dymond, C.C., Stinson, G., Rampley, G.J., Neilson, E.T., Carroll, A.L., Ebata, T., and Safranyik, L. 2008. Mountain pine beetle and forest carbon feedback to climate change. Nature, **452**: 987–990. doi:10.1038/nature06777.

Kurz, W.A., Shaw, C.H., Boisvenue, C., Stinson, G., Metsaranta, J., Leckie, D., Dyk, A., Smyth, C., and Neilson, E.T. 2013. Carbon in Canada's boreal forest — a synthesis. Environ. Rev. **21**: 260–292. doi:10.1139/er-2013-0041.

Lambert, M.-C., Ung, C.-H., and Raulier, F. 2005. Canadian national tree aboveground biomass equations. Can. J. For. Res. **35**: 1996–2018. doi:10.1139/x05-112.

Margolis, H., Sun, G., Montesano, P.M., and Nelson, R.F. 2015. NACP LiDAR-based biomass estimates, boreal forest biome, North America, 2005–2006. Oak Ridge National Laboratory Distributed Active Archive Center, Oak Ridge, Tennessee, U.S.A. Dataset available from http://daac/ornl.gov/. doi:10.3334/ORNLDAAC/1273.

McRoberts, R.E., and Westfall, J.A. 2014. Effects of uncertainty in model predictions of individual tree volume on large area volume estimates. For. Sci. **60**: 34–42. doi:10.5849/forsci.12-141.

Michaelian, M., Hogg, E.D., Hall, R.J., and Arsenault, E. 2011. Massive mortality of aspen following severe drought along the southern edge of the boreal forest. Glob. Chan. Biol. **17**: 2084–2094. doi:10.1111/j.1365-2486.2010.02357.x.

Montesano, P.M., Dubayah, R.O., Sun, G., Cook, B.D., Ranson, K.J., Naesset, E., and Kharuk, V. 2014. The uncertainty of biomass estimates from LiDAR and SAR across a boreal forest structure gradient. Remote Sens. Environ. **154**: 398–407. doi:10.1016/j.rse.2014.01.027.

Montesano, P.M., Rosette, J., Sun, G., North, P., Nelson, R.F., Dubayah, R.O., Ranson, K.J., and Kharuk, V. 2015. The uncertainty of biomass estimates from modeled ICESat-2 returns across a boreal forest gradient. Remote Sens. Environ. **158**: 95–109. doi:10.1016/j.rse.2014.10.029.

Næsset, E., Gobakken, T., Solberg, S., Gregoire, T.G., Nelson, R., Ståhl, G., and Weydahl, D. 2011. Model-assisted regional forest biomass estimation using LiDAR and InSAR as auxiliary data: a case study from a boreal forest area. Remote Sens. Environ. **115**: 3599–3614. doi:10.1016/j.rse.2011.08.021.

Neigh, C.S.R., Nelson, R.F., Ranson, K.J., Margolis, H.A., Montesano, P., Sun, G., Kharuk, V., Naesset, E., Wulder, M., and Anderson, H.E. 2013. Taking stock of circumpolar boreal forest carbon. Remote Sens. Environ. **137**: 274–287. doi:10.1016/j.rse.2013.06.019.

Nelson, R. 2010. Model effects on GLAS-based regional estimates of forest biomass and carbon. Intl. J. Remote Sens. **31**: 1359–1372. doi:10.1080/01431160903380557.

Nelson, R.F., Krabill, W., and Tonelli, J. 1988. Estimating forest biomass and volume using airborne laser data. Remote Sens. Environ. **24**: 247–267. doi:10.1016/0034-4257(88)90028-4.

Nelson, R., Parker, G., and Hom, M. 2003*a*. A portable airborne laser system for forest inventory. Photogramm. Eng. Remote Sens. **69**(3): 267–273. doi:10.14358/PERS.69.3.267.

Nelson, R., Valenti, M., Short, A., and Keller, C. 2003*b*. A multiple resource inventory of Delaware using airborne laser data. Bioscience, **53**: 981–992. doi:10.1641/0006-3568(2003)053[0981:AMRIOD]2.0.CO;2.

Nelson, R., Keller, C., and Ratnaswamy, M. 2005. Locating and estimating the extent of Delmarva fox squirrel habitat using an airborne LiDAR profiler. Remote Sens. Environ. **96**: 292–301. doi:10.1016/j.rse.2005.02.012.

Nelson, R., Boudreau, J., Gregoire, T.G., Margolis, H.A., Næsset, E., Gobakken, T., and Ståhl, G. 2009*a*. Estimating Quebec provincial forest resources using ICESat/GLAS. Can. J. For. Res. **39**: 862–881. doi:10.1139/X09-002.

Nelson, R., Ranson, K.J., Sun, G., Kimes, D.S., Kharuk, V., and Montesano, P. 2009*b*. Estimating Siberian timber volume using MODIS and ICESat/GLAS. Remote Sens. Environ. **113**: 691–701. doi:10.1016/j.rse.2008.11.010.

Nelson, R., Gobakken, T., Naesset, E., Gregoire, T.G., Ståhl, G., Holm, S., and Flewelling, J. 2012. Lidar sampling — using an airborne profiler to estimate forest biomass in Hedmark County, Norway. Remote Sens. Environ. **123**: 563–578. doi:10.1016/j.rse.2011.10.036.

Olson, D.M., Dinerstein, E., Wikramanayake, E.D., Burgess, N.D., Powell, G.V.N., Underwood, E.C., D'Amico, J.A., Itoua, I., Strand, H.E., Morrison, J.C., Loucks, C.J., Allnutt, T.F., Ricketts, T.H., Kura, Y., Lamoreux, J.F., Wettengel, W.W., Hedao, P., and Kassem, K.R. 2001. Terrestrial ecoregions of the world: a new map of life on Earth. Bioscience, **51**: 933–938. doi:10.1641/0006-3568(2001)051[0933:TEOTWA]2.0.CO;2.

Price, D.T., Alfaro, R.I., Brown, K.J., Flannigan, M.D., Fleming, R.A., Hogg, E.H., Girardin, M.P., Lakusta, T., Johnston, M., Mckenney, D.W., Pedlar, J.H., Stratton, T., Sturrock, R.N., Thompson, I.D., Trofymow, J.A., and Venier, L.A. 2013. Anticipating the consequences of climate change for Canada's boreal forest ecosystems. Environ. Rev. **21**: 322–365. doi:10.1139/er-2013-0042.

Roy, D.P., Boschetti, L., and Justice, C. 2006. Global mapping of fire-affected areas using multi-temporal MODIS data: the MCD45 product. *In* Proceedings of the 2006 IEEE International Geoscience and Remote Sensing Symposium. Vols. 1–8. pp. 4165–4168.

Simard, M., Pinto, N., Fisher, J.B., and Baccini, A. 2011. Mapping forest canopy height globally with spaceborne LiDAR. J. Geophys. Res. Biogeosci. **116**: G04021. doi:10.1029/2011JG001708.

Soja, A.J., Tchebakova, N.M., French, N.H., Flannigan, M.D., Shugart, H.H., Stocks, B.J., Sukhinin, A.I., Parfenova, E.I., Chapin, F.S., and Stackhouse, P.W. 2007. Climate-induced boreal forest change: predictions versus current observations. Glob. Planet. Change, **56**: 274–296. doi:10.1016/j.gloplacha.2006.07.028.

Ståhl, G., Holm, S., Gregoire, T.G., Gobakken, T., Næsset, E., and Nelson, R. 2011. Model-based inference for biomass estimation in a Lidar sample survey in Hedmark County, Norway. Can. J. For. Res. **41**: 96–107. doi:10.1139/X10-161.

Ståhl, G., Heikkinen, J., Petersson, H., Repola, J., and Holm, S. 2014. Sample-based estimation of greenhouse gas emissions from forests — a new approach to account for both sampling and model errors. For. Sci. **60**: 3–13. doi:10.5849/forsci.13-005.

Stinson, G., Kurz, W.A., Smyth, C.E., Neilson, E.T., Dymond, C.C., Metsaranta, J.M., Boisvenue, C., Rampley, G.J., Li, Q., White, T.M., and Blain, D. 2011. An inventory-based analysis of Canada's managed forest carbon dynamics, 1990 to 2008. Glob. Chang. Biol. **17**: 2227–2244. doi:10.1111/j.1365-2486.2010.02369.x.

Woudenberg, S.W., Conkling, B.L., O'Connell, B.M., LaPoint, E.B., Turner, J.A., and Waddell, K.L. 2010. The forest inventory and analysis database: database description and users guide version 4.0 for phase 2. USDA Forest Service, Rocky Mountain Research Station, Fort Collins, Colorado, Gen. Tech. Rep. RMRS-GTR-245.

Wulder, M.A., Dechka, J.A., Gillis, M.A., Luther, J.E., Hall, R.J., Beaudoin, A., and Franklin, S.E. 2003. Operational mapping of the land cover of the forested area of Canada with Landsat data: EOSD land cover program. For. Chron. **79**: 1075–1083. doi:10.5558/tfc791075-6.

Wulder, M.A., Kurz, W., and Gillis, M. 2004. National level forest monitoring and modelling in Canada. Prog. Plann. **61**: 365–381. doi:10.1016/S0305-9006(03)00069-2.

Wulder, M.A., White, J.C., Bater, C.W., Coops, N.C., Hopkinson, C., and Chen, G. 2012*a*. LiDAR plots — a new large-area data collection option: context, concepts, and case study. Can. J. Remote Sens. **38**: 600–618. doi:10.5589/m12-049.

Wulder, M.A., White, J.C., Nelson, R.F., Naesset, E., Ole Ǿka, H., Coops, N.C., Hilker, T., Bater, C.W., and Gobakken, T. 2012*b*. Lidar sampling for large-area forest characterization: a review. Remote Sens. Environ. **121**: 196–209. doi:10.1016/j.rse.2012.02.001.

Wulder, M.A., Coops, N.C., Hudak, A.T., Morsdorf, F., Nelson, R., Newnham, G., and Vastaranta, M. 2013*a*. Status and prospects for lidar remote sensing of forested ecosystems. Can. J. Remote Sens. **39**: S1–S5. doi:10.5589/m13-051.

Wulder, M.A., White, J.C., Cranny, M., Hall, R.J., Luther, J.E., Beaudoin, A., Goodenough, D.G., and Dechka, J.A. 2013*b*. Monitoring Canada's forests. Part 1: Completion of the EOSD land cover project. Can. J. Remote Sens. **34**: 549–562. doi:10.5589/m08-066.